- 1 Quantifying new versus old aerosol deposition in forest canopies: throughfall mass balance with
- 2 fallout radionuclide chronometry
- 3 Joshua D. Landis¹
- ¹Dartmouth College, 19 Fayerweather Hill Road, Hanover NH 03755 USA 4
- correspondence to joshua.d.landis@dartmouth.edu 5

7 **Abstract**

6

19

27

28

29

31

32

33

34

36

8 Net throughfall (NTF) measurements of the fallout radionuclides (FRNs) ⁷Be and ²¹⁰Pb confirm that the 9 atmosphere is a strong net source of particulate matter (PM) and trace metals (TMs) to a temperate

10 forest canopy, which retains nearly 60% of total wet and dry annual atmospheric flux of the FRNs (four 11 trees, three species, two sites, n=159). Estimation of dry deposition using a multiple regression

technique and predictors of precipitation depth and duration of the antecedent dry period agrees well 12

with ecosystem mass balance, with about 25% of both ⁷Be and ²¹⁰Pb annual flux deposited by dry 13

processes, and total FRN fluxes in reasonable agreement with regional soil inventories. In contrast to the 14

15 FRNs, other TMs, including Pb and Hg show large enrichments in throughfall which derive from processes

16 of internal ecosystem recycling such as PM resuspension, leaching from tree metabolic pathways, and

17 physicochemical weathering of non-foliar biological tissues of the tree canopy (collectively

18 'phyllosphere'). To estimate the contributions to net throughfall from these internal pathways, which

we term a change storage (ΔS), a new FRN canopy mass balance is derived based on the different half-

lives of ${}^{7}\text{Be}$ and ${}^{210}\text{Pb}$. Estimated ΔS for selected elements are: $SO_4=7\%$; ${}^{210}\text{Pb}=29\%$; $\Delta S=42\%$; ${}^{9}\text{Be}=10^{-2}$ 20

21 45%; Cd = 60%; Hg = 60%; Pb = 63%; Fe =79%; Al = 79%; P =91%. The balance of throughfall (1-ΔS)

22 represents new ecosystem input. Change in storage for all elements was strongly correlated with export of particulate carbon (FPOM) and dissolved organic carbon (DOC) from the canopy, indicating that 23

24 physicochemical transformation during residence within the canopy facilitates the release of metals

25

from storage. ΔS thus represents an emergent ecosystem property through which metal, carbon, and 26 hydrologic cycles may converge to determine the fate, reactivity, and timing of metal delivery to

underlying soils. The forest canopy represents a substantial reservoir of decade-aged PM and cannot be

assumed at steady-state with respect to ongoing atmospheric deposition, especially in the context of

changing atmospheric composition, e.g., declining industrial emissions of Pb and Hg.

30

Plain Language Summary

Particulate matter (PM) in the atmosphere contains nutrients and toxins that impact the health of both

humans and ecosystems. Understanding how PM is deposited to land from the atmosphere is

challenging, however, due to its very small size and complex composition. Here we develop a new

35 method using natural radioactive elements to better measure how much PM is deposited, well as the

timescales over which it recirculates between the atmosphere and land.

Deleted: precipitation

Deleted: secondary aerosol,

Deleted: trace metals (

Deleted:)

Deleted: including

Deleted: s

Deleted: PM

Deleted: release

1. Introduction

45

60

61

62

63

64

65

66

67

68

69

70

71

72

73

74

75

76

77

78 79

80

81

46 Forest vegetation covers over 30% of the earth's landmass and thus mediates the impacts of particulate 47 matter (PM) deposition on climate, ecosystem function, and human health (Bortolazzi et al., 2021; 48 Emerson et al., 2020; Farmer et al., 2021; Hosker and Lindberg, 1982; IPCC, 2021; Jiskra et al., 2018; 49 Johnson and Siccama, 1983; Lindberg et al., 1982; Lovett and Lindberg, 1984; McDowell et al., 2020; Van 50 Stan and Pypker, 2015; WHO, 2016, 2021). Despite regulating the composition of both the atmosphere and terrestrial ecosystems, however, the interaction of vegetation with PM and other atmospheric trace 51 52 metals (TMs) remains poorly understood. Even a basic understanding of mechanisms that regulate PM 53 uptake by vegetation remain elusive (Luo et al., 2019; Shahid et al., 2017; Zhou et al., 2021). As a result, 54 in part, current estimates for PM dry deposition in global chemical transport models vary across orders 55 of magnitude, underpredict direct observations by as much as 200%, omit fundamental processes such as resuspension, and lack verification by mass balance (Emerson et al., 2020; Farmer et al., 2021; Hicks 56 57 et al., 2016; Pryor et al., 2017; Saylor et al., 2019). Moreover, long residence times of PM in recirculation 58 at the earth surface prolong impacts of critical pollutants such as Hg and Pb, and their ultimate fate 59 remains unclear (Resongles et al., 2021; Wang et al., 2020). These uncertainties underscore a critical

need for <u>an</u> improved understanding of <u>atmosphere</u>-biosphere interactions.

the chemical species that can be measured (Farmer et al., 2021).

Two approaches are used for measuring PM and TM deposition to forest canopies, each with characteristic advantages and limitations (e.g., Draaijers et al., 1996). Micrometeorological approaches infer rates of deposition based on concentration gradients in air, or covariance of airborne concentrations with turbulence (e.g., eddy flux; Emerson et al., 2018; Laguionie et al., 2014; Obrist et al., 2021). These methods are critical insofar as they estimate deposition over large areas with in some cases resolution of PM by size, However, these results are dependent on assumptions regarding micrometeorological physics, do not provide information on PM composition, and ultimately lack verification by mass balance ("where did it go?"). The logistical demands of the micrometeorological methods are challenging to satisfy, as well, requiring long term deployment of instrumentation to dedicated research sites, and dependence on strong vertical concentration gradients (in the eddy gradient approach). For the eddy covariance method, the need for fast and selective detectors restricts

A complementary approach exploits canopy chemical mass balance by comparing precipitation collected under vegetated canopies (throughfall or TF) with paired bulk deposition measurements under open sky (openfall or OF). Positive net throughfall (NTF = TF- OF) results for most elements. The excess is conventionally attributed to some combination of washoff of dry deposition that has accumulated in the canopy during the preceding dry period and leaching/weathering from biological tissues of the canopy itself. No accommodation is made for long-term PM or TM storage in ecosystem components, however, and quantifying the contribution of dry deposition thus requires uncertain assumptions for distinguishing between these competing processes ("where did it come from?"; Lovett & Lindberg, 1984; Ulrich, 1983). Distinguishing these processes is critical for understanding ecosystem trace metal budgets, since they can represent either a novel external source via dry deposition of PM, or internal

82 83 recycling via either resuspended dust or leaching of biological materials (Avila and Rodrigo, 2004;

84 Lindberg et al., 1982).

85 One critical source of error in throughfall mass balance is the assumption that precipitation is a simple 86 and efficient process of 'washoff' that fully removes dry deposition that has accumulated during dry periods preceding the rain event (Bishop et al., 2020; Gandois et al., 2010; IAEA, 2009; Lovett and 87

88 Lindberg, 1984; USEPA, 2005). The canopy is thus assumed at steady-state, and no accommodation is 89 made for accumulation of PM or TMs over time, or for any change in storage within the canopy. Support

for precipitation as an efficient washoff process derives from the large enrichments of most elements

Deleted: PM-vegetation

Deleted: PM

Deleted: PM Deleted: aerosol

Deleted: PM

Deleted: and Deleted: with

Deleted: s, but r

Deleted:

Deleted:

Deleted: PM

103 residence times on the order of just days to weeks (Chamberlain, 1970; Miller and Hoffman, 1983); and 104 washing of natural vegetation which shows exponential declines in rates of metal extraction (Avila and 105 Rodrigo, 2004; Shanley, 1989). This conceptualization of washoff also aligns with the 'Lotus effect', 106 which is the efficient self-cleaning of leaves by raindrops due to their hydrophobic waxy cuticle 107 (Barthlott and Neinhuis, 1997). 108 On the other hand, it is well documented that a range of atmospheric metals and metalloids accumulate 109 continuously in vegetation during exposure to the atmosphere. These include the natural fallout radionuclides (FRNs) ⁷Be and ²¹⁰Pb (Landis et al., 2014; Sumerling, 1984), anthropogenic fission products 110 including ⁹⁰Sr (Yamagata et al., 1969), ¹³¹I (Yamagata, 1963), ¹³⁷Cs and others (Kato et al., 2012; Russell et 111 112 al., 1981), TMs including Al, Pb, and Hg (Landis, 2024a; Rea et al., 2001, 2002; Wyttenbach and Tobler, 113 1988), and oxoanions AsO₃, SeO₃, and CrO₄ (Landre et al., 2009). Moreover, this accumulation continues 114 unabated in senescent vegetation, indicating that PM and TM uptake occurs independent of leaf 115 physiology and is thus unambiguously atmospheric in origin. The foliar metal residence times of Hg, ⁷Be, 116 ²¹⁰Pb, and ¹³⁷Cs have been shown by various means to exceed 700 days, which is generally longer than 117 the lifetime of the foliage itself. This demonstrates strong coupling of atmospheric metals to the carbon 118 cycle (Graydon et al., 2009; Kato et al., 2012; Landis et al., 2014). 119 In the case of Hg, although its occurrence in the atmosphere is regulated by gaseous elemental mercury 120 (GEM) rather than by PM, recent measurements nonetheless show that long-lived non-foliar materials 121 of the forest canopy including bark, lichen, moss, and foliage (collectively "phyllosphere") collectively 122 retain many times the annual Hg flux on an areal basis (Wang et al., 2020), This shows that GEM 123 becomes particle-bound during its residence in the phyllosphere, and also that surfaces other than 124 foliage therefore play a dominant role in canopy and ecosystem mass balances of Hg and other TMs 125 (Obrist et al., 2021). Stable isotopes of both Hg and Pb reveal that legacy anthropogenic emissions 126 continue to dominate contemporary atmospheric deposition, for example, despite large reductions in 127 both emissions and measured rates of deposition (Farmer et al., 2010; Resongles et al., 2021; Taylor et 128 al., 2022; Yang and Appleby, 2016). These legacy TM sources remain enigmatic but might include 129 resuspended dust from surrounding soils and roads, or release from storage in living and dead surfaces 130 of the phyllosphere. Resolving multiple processes that regulate accumulation, storage, and re-131 suspension of diverse TMs in terrestrial ecosystems, and their contributions to depositional budgets, 132 remains a challenge to biogeochemical research. This is especially important in the context of changing 133 global emissions of, e.g., Hg and Pb, since the forest cannot be assumed at steady-state with respect to 134 contemporary deposition. The natural fallout radionuclide (FRN) tracers ⁷Be and ²¹⁰Pb provide a novel and emerging perspective on 135 136 PM metal cycling. The FRNs have been shown to accumulate in vegetation primarily by wet denosition rather than dry as widely presumed (Landis, 2024a; Landis et al., 2014). This distinction is important 137 138 because approximately 90% of PM removal from the atmosphere occurs by wet processes (in 139 continental climates), and the accumulation of FRNs in forest canopies might thus reflect a quantitative view of PM cycling from the atmosphere. The FRNs 7Be and 210Pb are secondary aerosols produced in 140 141 the atmosphere from gaseous precursors by cosmogenic spallation of N2 and O2 or radiogenic decay of ²²²Rn, respectively, with identical PM activity-size distributions (mean aerodynamic diameters) of ca. 0.5 142

that are observed in throughfall, experimental dry applications of PM to vegetation which show

102

143

144

145

146

2016).

Deleted: ,

Deleted: ,

Deleted: trace metals (

Deleted:)

Deleted: is

Deleted: PM

Deleted: PM

Deleted: This demonstrates long

Deleted: residence times for diverse PM metals in the phyllosphere, and

Deleted: also that

Deleted: may

Deleted: Further, s

Deleted: PM

Deleted: PM

μm (Gründel and Porstendörfer, 2004; Winkler et al., 1998). FRNs are widely exploited as tracers of

metals in long-range transport (Koch et al., 1996; Lamborg et al., 2013; Landis et al., 2021a; Liu et al.,

other PM components of broad interest including PM2.5, black carbon, sulfate, and anthropogenic trace

162 The FRNs hold special power as PM tracers through two consequences of their radioactive decay. First, 163 their accumulation in the terrestrial environment is limited such that their occurrence can be 164 unambiguously traced directly to an atmospheric origin. Second, their characteristic rates of decay can 165 be exploited to explicitly measure timescales of their deposition and redistribution. For example, ⁷Be 166 and ²¹⁰Pb are produced in the atmosphere with a typical activity ratio on the order of 10. In vegetation exposed to ongoing atmospheric deposition, both FRNs accumulate with time but the $^7\mathrm{Be}:^{210}\mathrm{Pb}$ ratio 167 decreases due to their differing half-lives. After one year of exposure foliage has ratios of 2-3. With its 168 169 short half-life of 54 days, ⁷Be records the PM-vegetation interaction over event-based timescales, 170 whereas ²¹⁰Pb records longer-term storage, resuspension, and recycling of PM deposition over subannual to decadal timescales (Landis et al., 2021a; Landis et al., 2021b) . 171

Here we use FRN chronometry in a throughfall mass balance approach to resolve processes and timescales that govern the interactions of PM and atmospheric TMs with forest canopies. We first review contemporary approaches to throughfall mass balance and then derive a new expression using

FRNs to distinguish the initial absorption of PM during deposition from later release from canopy storage. We confirm that ⁷Be and ²¹⁰Pb are not systematically fractionated and that the ⁷Be:²¹⁰Pb ratio in

throughfall is primarily a measure of PM age. We then extend our throughfall mass balance approach to link the FRNs and other major and trace elements (MTEs) to canopy export of dissolved organic carbon

179 (DOC) and fine particulate organic matter (FPOM).

1.1. Throughfall mass balance

180

181

182

183

184

185 186

187188

189

190

191

192

193

194

195

The conventional throughfall mass balance includes two pathways by which PM enters and leaves the canopy. Inputs to the canopy by bulk wet deposition (W) or dry deposition (D) must be balanced by exports via wet throughfall (T) and any exchange with the canopy (C) via leaching (+) or absorption (-):

$$W+D=T\pm C$$
 Eq. 1

Bulk deposition (*W*) is measured under open sky adjacent to the forest where it may also be called openfall (*OF*). Net throughfall (*NTF*) is the arithmetic difference between deposition under the canopy and open sky:

$$NTF = T - W = D \pm C$$
 Eq. 2

W and T are easily measured. The challenge in estimating D by mass balance then remains to distinguish contributions of C. Two approaches have been proposed. The more common is the 'filtering' approach (Staelens et al., 2008; Ulrich, 1983; Yoshida and Ichikuni, 1989) where an index element is used to apportion dry deposition of the target element, D_i. The index element, typically Na or Al, is assumed to have identical rates of dry deposition as the target element (Eq. 3) but no metabolic contribution from the canopy. This assumption implicitly presumes similar PM size distributions, and thus sources with respect to secondary or primary emission, insofar as PM size controls rates of dry deposition (Jaenicke, 1980).

196 1980).
197
$$\frac{D_i}{W_i} = \frac{D_{Na}}{W_{Na}}$$
 Eq. 3

198 With C_{No} =0, dry deposition of an element of interest can be calculated as follows:

$$D_i = W_i \cdot \frac{T_{Na} - W_{Na}}{W_{Na}} = W_i \cdot (EF_{Na} - 1)$$
 Eq. 4

Here, EF_{Na} represents the Na enrichment factor =T/W. Following the calculation of D_i by Eq. 4, C_i can be solved from Eq. 2. By this approach any EF_i greater than EF_{Na} yields a positive C_i , which represents

Deleted: deposition and interaction

leaching from the canopy. Any EF_i less than $EF_{N\sigma}$ yields negative C_i , which represents a net loss to the canopy by absorption.

A second approach to describing the canopy interaction uses multiple regression of individual storm events to estimate rate constants for specific canopy processes (Lovett and Lindberg, 1984; Rea et al., 2001; Wu et al., 1992):

$$NTF = T - W = D + C = \beta_1 A + \beta_2 P$$
 Eq. 5

The coefficient β_1 represents the rate of dry deposition to the canopy [Bq m² d¹ or µg m² d¹] and A is the duration of the antecedent dry period preceding the storm event [days]. The coefficient β_2 represents either canopy leaching or absorption [Bq or µg m² cm²] with P the precipitation total [cm]. Biotic leaching and abiotic exchange (desorption, dissolution) can be distinguished only by a priori assumptions based on elemental chemistry, and that one must dominate the other, for example that base cations K, Ca, Mg, etc., are strongly cycled through leaf tissue and are thus derived primarily from leaching, whereas trace metals, e.g. Pb, are not appreciably cycled and are thus dominated by canopy absorption (Lovett and Lindberg, 1984).

An important advantage to this approach is that, provided sufficient measurements, additional explanators might be added to the multiple regression to understand effects from other environmental factors such as seasonality, tree species, precipitation pH, dissolved organic carbon (DOC), or fine particulate organic matter (FPOM).

1.2. FRN mass balance: change in canopy storage

The observed accumulation of FRNs and TMs in foliage and long-lived tissues of the phyllosphere requires that canopy exchange must accommodate a change in storage, if previously deposited PM is later susceptible to weathering processes and export from the canopy in subsequent rainfall over some characteristic timeframe. We can distinguish this change in storage as a separate term in mass balance as follows based on different characteristic timescales:

$$T = W + D \pm (C + \Delta S)$$
 Eq. 6

Analogous to the use of an index element for dry deposition in the filtering approach, we propose to use ⁷Be as an index of canopy storage. Beryllium is highly reactive to natural surfaces but due to its short half-life, ⁷Be cannot record long-term storage. In contrast, the longer-lived ²¹⁰Pb persists to record PM fate over annual to decadal timescales. The similar occurrence and behaviors of ⁷Be and ²¹⁰Pb, but different half-lives, thus allow us to distinguish instantaneous canopy exchange (absorption or leaching) from a subsequent change in storage. Storage is thus defined as occurring over timescales that are long relative to the ⁷Be half-life (54 days). We assume that the ⁷Be:²¹⁰Pb flux ratio is constant through time, but acknowledge that short-term variability and long-term decadal trends in ²¹⁰Pb deposition may require future attention (Landis et al., 2021a; Winkler and Rosner, 2000).

We <u>now</u> write two equations to solve for one unknown, ΔS :

$$T_{Be} = W_{Be} + D_{Be} \pm C_{Be}$$
 Eq. 7
$$T_{Pb} = W_{Pb} + D_{Pb} \pm (C_{Pb} + \Delta S)$$
 Eq. 8

Eq. 7 ignores radioactive decay, with an assumption that the residence time of dry deposition in the canopy is very short (days) relative to the ⁷Be half-life. This assumption is re-evaluated in *Sect. 3.4.* Based on their congruent interactions with natural vegetation and particulate matter (Landis, 2023; Landis et

Deleted: exchange

Deleted: their

Formatted: Superscript

Formatted: Superscript

Formatted: Superscript

al., 2014, 2016, 2021b, 2024a), we next assume that ⁷Be and ²¹⁰Pb have similar canopy interactions and that for both *C* is an equivalent fraction of total wet+dry deposition (Eq. 9).

$$\frac{c_{Be}}{W_{Be}EF_{Na}} = \frac{c_{Pb}}{W_{Pb}EF_{Na}}$$
 Eq. 9

This allows us to combine Eq. 7 and Eq. 8, with both D and C terms cancelling. We then solve for ΔS as follows, by which we attribute any throughfall excess in 210 Pb relative to 7 Be to a change in storage:

$$\Delta S = T_{Pb} - T_{Be} \cdot \frac{W_{Pb}}{W_{Be}}$$
 Eq. 10

For species with a gaseous phase such as Hg or SO_4 , we cannot assume a constant D/W ratio as in Eq. 3.

In these cases, we use an alternative mass balance by directly estimating dry deposition via multiple regression (β_1) for both ⁷Be and, e.g., Hg, as follows:

$$\Delta S_{Hg} = Hg_{NTF*} - Be_{NTF*} \cdot \frac{w_{Hg} + D_{Hg}}{w_{Be} + D_{Be}}$$
 Eq. 11

The term Hg_{NTF^*} represents NTF without contribution from C, i.e., $Hg_{NTF^*}=T_{Hg}-W_{Hg}-D_{Hg}$.

Finally, calculating a change in storage acknowledges that a process of exchange occurs within the canopy. Some fraction of new wet and dry deposition is retained by the canopy, while some fraction of previous deposition is released from storage. The proposed mass balance thus provides a new perspective on PM and TM deposition, new versus old. ΔS quantifies the old, and the fraction new follows from mass balance:

$$Hg_{new} = T_{Hg} - \Delta S_{Hg}$$
 Eq. 12

2. Methods

2.1. Site and tree characteristics

We measured 156 samples of throughfall under mature canopies of two tree species at each of two sites. The Beaver Meadow (BM) site in Sharon, Vermont (104 km², population =1500) sits at an elevation of 502 m in mixed forest of sugar maple, red oak, American beech, white pine, and poplar, with understory of striped maple and hornbeam. Annual precipitation averages 117 cm y¹ for the past 30 years (PRISM 2014). The site is underlain by green schists of the Waits River series and thin glacial till which leads to development of well-drained soils typically classified as Inceptisol. Throughfall was collected under red oak (*Quercus rubra*; diameter at breast height, dbh =28 cm) and white pine (*Pinus strobus*; dbh = 59 cm) in the forest interior, and openfall was collected within 50 m in an adjacent forest gap. The Shattuck Observatory (SO) site is located 18 km distant in Hanover, New Hampshire (130 km², population =8500), in the semi-urban forest of the Dartmouth College Park at an elevation of 165 m. Annual precipitation averages 101 cm y¹ (PRISM 2014). The SO site is underlain by mafic volcanics of the Ammonoosuc series with frequent outcrops along this ridgeline site (Schumacher, 1988). Throughfall was collected under red oak (dbh = 53 cm) and Norway spruce (*Picea abies*; dbh = 60 cm) at the forest edge, with openfall collected within 50 m in the adjacent clearing where we have previously reported a long-term timeseries of atmospheric deposition (Landis et al., 2021a; Landis et al., 2021b).

The sampled trees represent a range of foliar ages and characteristics that may influence FRN activities and MTE concentrations. Red oak is deciduous and sheds most leaves annually after ca. 6 months of growth (May-October); however, some remain on branches following abscission through the following winter (a phenomenon called marcescence). White pine retains needles for 1.5-2 years. Norway spruce retains needles for up to 5-8 years (Reich et al., 1996). Leaf area index (LAI) at each throughfall site was

Deleted: cases of

Deleted: aerosols

Deleted: aerosol

Deleted: is

289 estimated over a 30° zenith angle using hemispheric photos and the software package Hemisfer 290 (Schleppi et al., 2007; Thimonier et al., 2010). Measured LAI are as follows: BM oak (leaf off) =0.9 ±0.3, BM oak (leaf on) =3.1 ± 0.5 , BM pine =2.79 ± 0.14 , SO oak (leaf off) 1.13 ± 0.4 , SO oak (leaf on) =5.9 ± 0.6 , 291 292 SO spruce = 4.52 ± 0.16 . 293 2.2 Sample collection and filtration 294

Each openfall and throughfall precipitation sampler consisted of 4 tandem polyethylene open collectors 295 (area =650 cm² each, depth=40 cm; cumulative projected area = 0.26 m²) mounted to a PVC post at a 296 height of 1.5 m above ground. Total collector surface area to projected ground area (surface area index) 297 =5.2 (e.g., Hicks, 1986). At each site samplers were located at the same aspect relative to the sampled 298 tree stem, under the midpoint of the tree crown to avoid dripline or stem effects. Collectors were 299 deployed prior to, and retrieved following, individual rain and snowstorms. Upon retrieval an aliquot 300 was immediately removed for measurement of operationally-dissolved major and trace elements 301 (MTEs) and DOC. This aliquot (a0) was filtered with a 0.45 µm Nylon filter (Fisher Scientific), the first 1 302 mL discarded, the next 5 mL used to rinse an acid-washed polyethylene vial and discarded, and a final 20 303 mL retained and acidified to 2% HCl (Optima grade). Sample pH was then measured in the bulk sample 304 with dual ROSS-type electrodes (Thermo Scientific), calibrated daily with fresh, low ionic strength buffer. 305 Bulk samples were then passed through a 1 mm polypropylene screen or hand-picked to remove coarse 306 debris and then filtered to tared 0.5 µm quartz fiber filters (QFF; Advantech QR-100) to remove an 307 insoluble fine particulate organic fraction (FPOM). The filtrate was acidified to 2% HCl with concentrated 308 acid (Trace Metal grade), and the acidified sample in turn was used to rinse and recover metals

310 FPOM on QFF filters was extracted sequentially using 2% HCl and reverse aqua regia (9:3 HNO₃:HCl, plus 311 0.2 mL BrCl) to estimate MTE solubility and to distinguish fluxes of dissolved (d.Pb, etc.), soluble, and

312 total <u>JM</u> deposition. The acid-soluble fraction (s.Pb, etc.) is the sum of dissolved and 2% HCl extraction. The total fraction (t.Pb, etc.) is the sum of dissolved, 2% HCl, and aqua regia fractions. The acid soluble 313 fraction is considered environmentally relevant (Lindberg and Harriss, 1981; Mahowald et al., 2018).

absorbed to the sample collection train and collector surfaces.

315 From dissolved and FPOM fractions we calculate distribution coefficients (K_D) as follows, where V is total sample volume (mL) and M is FPOM mass (g): 316

$$K_D = \frac{d.Pb/V}{(t.Pb-d.Pb)/M}$$
 Eq. 13

Enrichment factors of MTEs with respect to upper continental crust (EFcrustal) were calculated from 318 319 dissolved fractions in OF collections to maintain comparability the prior works (Duce et al., 1975; 320 Gandois et al., 2010; Taylor and McLennan, 1995):

$$EF_{crust} = (M_i/Al)_{OF}/(M_i/Al)_{crust}$$
 Eq. 14

2.3. Sample Analysis

309

314

317

321

322

330

323 FRNs were measured by gamma spectrometry following preconcentration by MnO₂ co-precipitation, 324 with yields averaging 88 ±15% for Be and 88 ±16% for Pb (mean ±SD). A workflow schematic is 325 illustrated in Fig. S1, and details are given elsewhere (Landis et al., 2012, 2021). MTEs were measured by 326 inductively-coupled plasma optical emission spectrometry (ICPOES; Spectro ARCOS) operated in axial 327 view. Low-level trace elements including As, Cd, Co, Cr, Cu, Fe, Pb, and V were measured by ICP triple-328 quadrupole mass spectrometry (ICPMS-QQQ; Agilent 8900) in the Dartmouth Trace Element Analysis 329 Core Facility (TEA Core). Reference material NIST1643f was used for quality control, with recoveries

Deleted: and

Deleted: aerosol

Deleted: d

Formatted: Not Highlight

Deleted: D

Deleted: are

within 95-105% for all analytes. Total Hg was measured by double amalgamation purge-and-trap atomic

- 336 fluorescence (Brooks Rand Merkx-T, Model III), where samples preserved in 2% HCl were oxidized by
- 337 reaction with 1% v/v BrCl at room temperature for 24 hours and then reduced to Hg_0 by addition of
- 338 SnCl₂ and hydroxylamine immediately prior to analysis. Reference material NIST1641e was used for Hg
- 339 quality control, with recovery of 10 pg averaging 97 ±8% (mean ±SD; n=48). Sample recovery spikes
- 340 averaged 97 ±6% (n=9). Dissolved organic carbon (DOC) was measured by automated combustion of
- acidified samples (General Electric); see also Hou et al. (2005) and Gandois et al. (2010).

2.4. Statistical analyses

342

- 343 Statistical analyses were performed in JMP Pro 16.0. Data were transformed to achieve normal
- 344 distributions and equal variances. For NTF which includes positive and negative values, this required
- transform of the form $\log_{10}(x+n)$ with n selected to scale all values >0. Our multiple regression approach
- 346 is described in more detail elsewhere (Landis et al., 2021a). We observe Bonferroni correction for
- 347 describing significance of multiple regression parameters but presented p-values do not include this
- 348 correction since the number of explanators are shown for each regression.

349 2.5. Literature review

- 350 Throughfall enrichment factors were compiled from the following literature sources (Ali et al., 2011;
- 351 Atteia and Dambrine, 1993; Avila and Rodrigo, 2004; Böhlke and Michel, 2009; Bringmark et al., 2013;
- 352 Demers et al., 2007; Eisalou et al., 2013; Forti et al., 2005; Fu et al., 2010; Gandois et al., 2010; Graydon
- 353 et al., 2008; Grigal et al., 2000; Henderson et al., 1977; Hou et al., 2005; Huang et al., 2011; Iverfeldt,
- 354 1991; Karwan et al., 2016, 2018; Kolka et al., 1999; Kopáček et al., 2009; Landre et al., 2009; Larssen et
- al., 2008; Lawson and Mason, 2001; Lindberg and Harriss, 1981; St. Louis et al., 2001, 2019;
- 356 Mahendrappa, 1987; Małek and Astel, 2008; Matschullat et al., 2000; Michopoulos et al., 2005, 2018;
- Oziegbe et al., 2011; Petty and Lindberg, 1990; Rea et al., 2001; Rehmus et al., 2017; Rodrigo et al.,
- 358 1999; Schwesig and Matzner, 2000; Skrivan et al., 1995; Sohrt et al., 2019; Stachurski and Zimka, 2000;
- 359 Tan et al., 2019; Ukonmaanaho et al., 2001; Wang et al., 2020; Wilcke et al., 2017; Zhang and Liang,
- 360 2012).

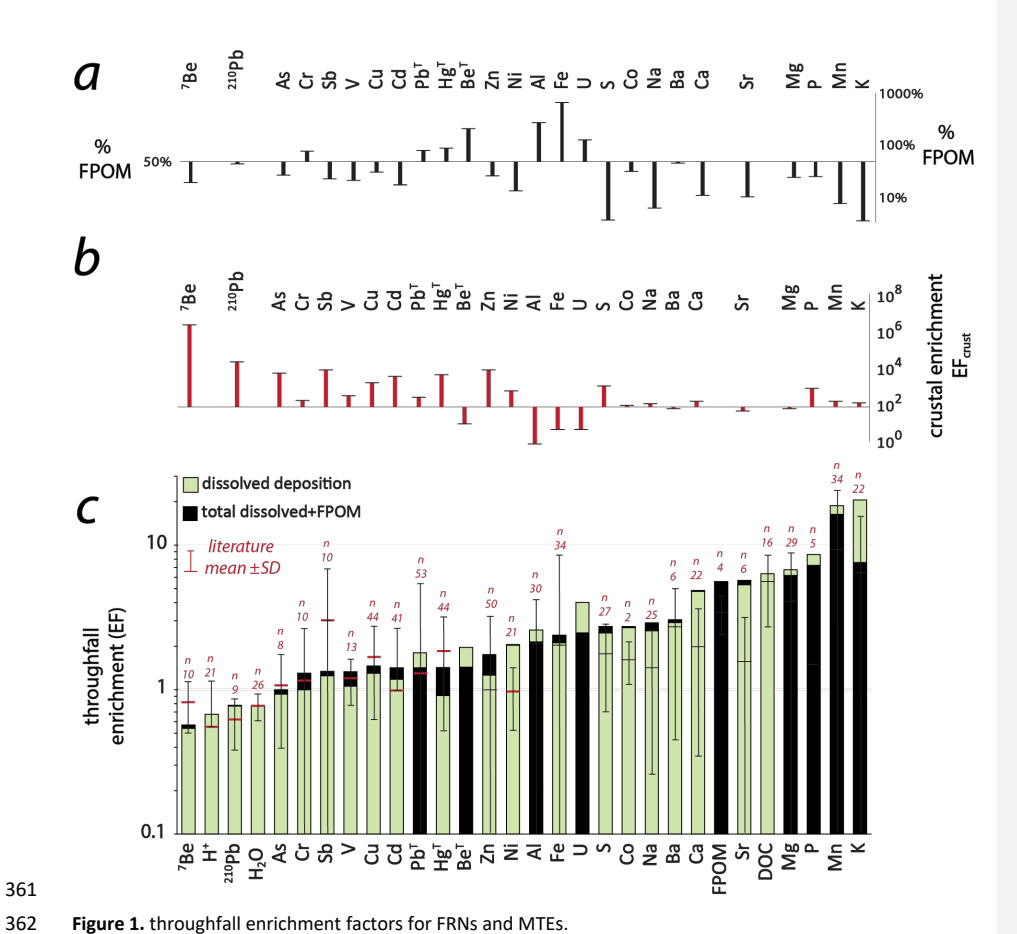


Figure 1. throughfall enrichment factors for FRNs and MTEs.
(a) % increase in throughfall flux when including a fraction extracted from fine particulate organic matter (FPOM); (b) crustal enrichment factors, where EF_{crustal} = [M/Al]_{OF}/[M/Al]_{crust}. (c) Median flux-based throughfall enrichment factors (EFs) for this study shown in bars. Note log₁₀ scaling. Line and whiskers show means and standard deviations compiled from literature sources, with number of experiments indicated as *n* (see *Methods*).

3. Results

3.1. FRN mass balance in the forest canopy

Throughfall enrichment factors and the partitioning of FRNs and MTEs to FPOM are shown in Fig. 1. Throughfall measurements including rainfall interception, FPOM, and DOC concentrations are shown in Fig. 52. The studied tree canopies typically intercept (retain) 20% of precipitation. DOC and FPOM are greatly increased through the canopy with TF concentrations in ranges of 1-10 µg mL⁻¹ and 10-100 µg

Deleted: \$1

376 mL⁻¹, respectively. Throughfall mean pH values for the seasons summer through winter were 5.29, 5.36, 377 4.98, and 4.86, respectively. Effect of the canopy on throughfall pH was variable (Fig. 53). The canopy Deleted: 52 378 was a net sink for H^+ in summer for each of spruce, pine, and oak [p<0.05]. On an annual basis, oak was 379 a net sink at both sites but both pine and spruce were net sources of H⁺. 380 Flux-based throughfall enrichment factors (EFs) for 7 Be and 210 Pb were 54.7 $\pm 0.3\%$ and 75.9 $\pm 1\%$, 381 respectively (±SE), significantly lower than 1 and thereby demonstrating that the canopy is an 382 unambiguous net sink for FRNs in wet deposition. ⁷Be shows stronger absorption than either H⁺ or H₂0, 383 which demonstrates its strong preferential absorption by the canopy. Only the following showed EFs less than 1: ⁷Be < H⁺ < ²¹⁰Pb < H₂O < As. All other MTEs showed a net gain through the canopy due to 384 385 some combination of dry deposition during the antecedent dry period, leaching from biological tissues, 386 or weathering from storage in the phyllophere. Putative reference elements expected to have minor 387 leaching contributions such as AI, Fe, U and Na showed moderate gains from the canopy, with EFs in the 388 range of 2-3. The following trace metals showed EFs less than these reference elements, which nominally indicates net sorption to the canopy: Cr, Sb, V, Cu, Cd, Pb, Hg, ⁹Be, Ni and Zn. Alkaline and 389 390 nutrient elements showed much larger EFs than reference elements, indicating strong net gains from 391 the canopy: Co, Ba, S, Ca, Sr, Mg, P, C, Mn and K, as well as DOC and FPOM. 392 Crustal enrichment factors (EF_{crust}) in the range of 10²-10³ indicate that <u>JF</u> metals are generally of Deleted: PM 393 anthropogenic atmospheric origin, whereas values ~1 confirm a terrestrial dust source for Al. Fe, and U 394 (Duce et al., 1975; Fig. 1b). EF_{crust} does not strictly identify atmospheric PM however, since values in the 395 range of 10² for alkaline elements can also reflect the high solubility of these elements and their 396 extraction from biological tissues of the phyllosphere during rainfall. Among tree species, spruce displayed lowest EFs for ⁷Be and ²¹⁰Pb (highest interception), but higher EFs 397 398 than either oak or pine for most elements [p<0.05]. By site, both spruce and oak at the SO site showed 399 higher EFs for ⁹Be, Ni, Sb, V and Zn, demonstrating a site effect for these elements which could be 400 related to higher pollutant loads near a higher population density, or alternatively to underlying mafic 401 lithology at this site [p<0.05]. By contrast, there were no species or site effects for the heavily cycled 402 elements Ca, Mg, K, P or Mn, or for metals including Cd, Cu, Hg, Pb, or U [p>0.05]. Tree species were 403 compared only during deciduous leaf-on months. 404 3.2. Interpreting canopy processes from FRN throughfall concentrations 405 Throughfall EFs evaluated on an annual basis described above show that the FRNs absorb strongly and 406 that the canopy is therefore a strong sink for secondary aerosol metals. For further insights into the 407 balance of processes acting to retain and release FRNs within the canopy at the event-scale, we also 408 evaluated the concentrations of FRNs as a function of precipitation depth for individual storms. Below 2 409 cm of precipitation both ⁷Be and ²¹⁰Pb concentrations in TF are generally greater than 100% of 410 concentrations in OF, and in some cases more than 300% higher than incident precipitation. This 411 indicates that net release of FRNs is the dominant process at low precipitation totals, which we attribute to the removal of dry-deposited PM which was deposited during the antecedent dry period (Fig. 2a). 412 Deleted: aerosol Deleted: were Beyond 2 cm of precipitation the concentrations of both ⁷Be and ²¹⁰Pb are lower than openfall, 413 indicating that the canopy transitions to a net sink with increasing precipitation depth. This suggests that 414 415 at some threshold amount of precipitation, susceptible dry-deposited PM is fully removed, and wet Deleted: aerosol 416 deposited PM continue to be absorbed by the canopy. The unambiguous net sorption of wet-deposited **Deleted:** aerosols 417 PM is clear when concentrations are converted to fluxes (by multiplication with precipitation depth; Fig. Deleted: aerosols

2b). At highest precipitation totals >6 cm there is some suggestion that sorption capacity of the canopy

may be exhausted and FRN yields from the canopy begin to increase, but data are too few for a <u>confident</u> interpretation.

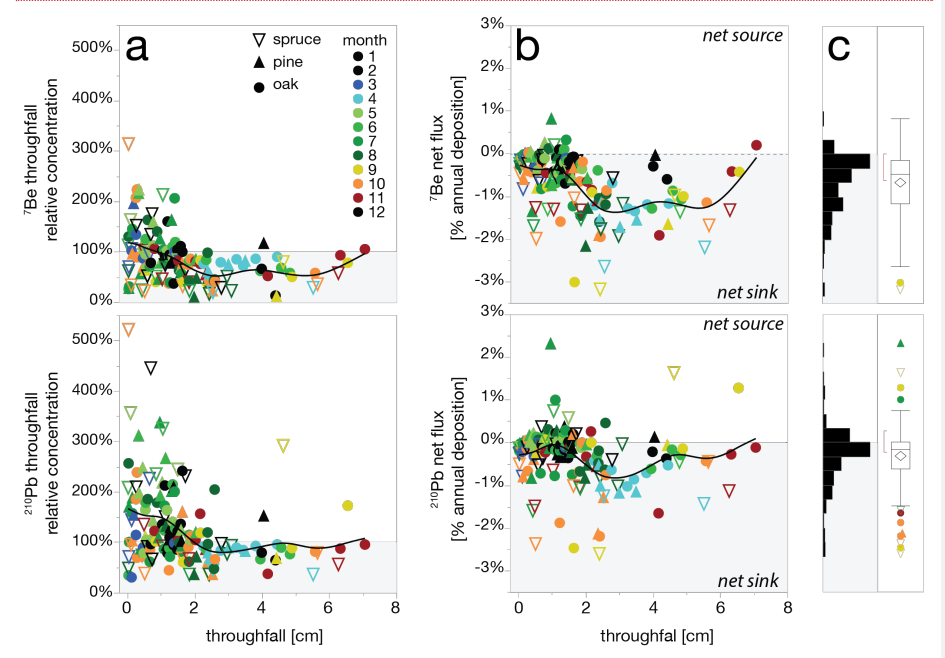


Figure 2. relative concentrations of ⁷Be or ²¹⁰Pb in throughfall versus openfall (EF=TF/OF).

(a) Oak is shown with circles, pine with triangles, spruce with open triangles. Black lines show a spline best-fit.

(b) net throughfall fluxes (NTF) of ⁷Be and ²¹⁰Pb as a percentage of total annual deposition. (c) histograms of ⁷Be and ²¹⁰Pb net flux.

3.3. Throughfall ⁷Be:²¹⁰Pb ratios as a metric of PM age

²¹⁰Pb is systematically biased to higher yields than ⁷Be despite the same patterns in canopy interactions, and as a result ⁷Be;²¹⁰Pb ratios are significantly lower in throughfall versus openfall (Fig. 2a, Fig. 53). Mean throughfall ⁷Be;²¹⁰Pb ratios across all species averaged 10.3 ±0.3 versus mean openfall of 14.8 ±0.5 [mean ±SE]. Throughfall for each tree species was significantly lower than paired openfall measurements [p<0.0001]. There was no correlation between throughfall pH and the ⁷Be;²¹⁰Pb ratio that might indicate discrimination of the FRNs through aqueous chemistry [R²=0.001, p=0.80; Fig. 53b]. We next used multiple regression to identify independent explanators on throughfall ⁷Be;²¹⁰Pb ratios and to quantify their independent effects on ⁷Be;²¹⁰Pb; we report independent effects as the % of total variance explained by each variable [in brackets] (Fig. 54). A predictive model for ⁷Be;²¹⁰Pb showed these significant explanators: species [22%], season [12%], and ⁷Be;²¹⁰Pb ratio of incident precipitation [9%] [R²= 0.42]. Adjusted for season and incident ratio, ⁷Be;²¹⁰Pb ratios among species increased in order: spruce (7.9 ±0.6)^A < pine < (9.5 ±0.6)^B oak (11.9 ±0.5)^C; values not sharing the same letter are significantly different [p<0.05]. Adjusted for both species and incident ratio, seasonal ratios increased in order: autumn (7.6)^A < summer (9.9)^B < winter (10.5)^{BC} < spring (11.3)^C. Both species and seasonal

Deleted: clear

Deleted: S2

Deleted: S2b

Deleted: S3

Deleted: .

453 patterns are consistent with the impact of tree phenology on long-term storage of ²¹⁰Pb, with the higher

LAI and older foliage of conifers storing larger reservoirs of ²¹⁰Pb, which is exported in small amounts 454

455 during subsequent storms.

The strongest discrimination between ⁷Be and ²¹⁰Pb appears to be their characteristic half-lives, in 456

457 absence of any evidence for impacts by environmental factors. There was no effect on ⁷Be:²¹⁰Pb from

458 antecedent dry period [R²=0.01, p=0.27], suggesting no discrimination in dry deposition between ⁷Be

and ²¹⁰Pb. There was no positive correlation between rainfall depth and ⁷Be:²¹⁰Pb [R²=0.03, p=0.42], in 459

460 contrast to OF where a strong positive correlation reflects the washout-rainout transition (Landis et al.,

461 2021). Importantly, there were no significant effects from factors that might indicate discrimination

between Be and Pb aqueous chemistries including: pH [p=0.32], $log_{10}(K_D)$ for either ⁷Be [p=0.34] or ²¹⁰Pb

462

463 [p=0.18], FPOM [p=0.29], DOC [p=0.47], or any MTE concentrations, fluxes, net fluxes, or enrichment

464 factors [p>0.05].

465

470

3.4. Multiple-regression mass balance to quantify dry deposition

466 We used multiple-regression mass balance to quantify the independent influences of wet and dry

467 deposition and canopy interactions that determine net throughfall (NTF) of the FRNs (Eq. 5). Overall

468 model fits for NTF are good for both ${}^{7}\text{Be}$ [R²=0.49, p<0.0001] and for ${}^{210}\text{Pb}$ [R²=0.30, p<0.0001] (Fig. 3).

Both ^7Be and ^{210}Pb show positive effects with antecedent dry period (θ_1) [p<0.05], and inverse effects 469

from precipitation depth (θ_2) apparent from Fig. 2 [p<0.05]. For ⁷Be the dry deposition rate (θ_1) is

471 equivalent to 213 ±53 Bg m⁻² per year or 13 ±4% of total annual deposition, (assuming that all dry

472 deposition is fully removed by subsequent storms). The multiple regression dry deposition estimate

473 does not incorporate ⁷Be decay that occurs during the antecedent period. However, with a decay rate of

474 1.3% per day, and median antecedent period of 7 days (mode of 2 days), underestimation of 7Be dry

475 deposition by ignoring radioactive decay is likely <10% of estimated dry deposition or <20 Bq m⁻² y⁻¹, For

 $^{210}\text{Pb},$ θ_{1} is equivalent to 19 ±6 Bq m $^{\text{-2}}$ per year or 15 ±5% of total annual deposition. 476

477 It is important to observe from Fig. 2 that dry deposition is not fully removed from the canopy by

478 subsequent rainfall since throughfall FRN concentrations may be higher than incident precipitation for

479 up to 2 cm of precipitation. During and following rain events it is thus likely that a complex exchange is

480 occurring at the leaf surface between wet and dry deposited PM, and both components are likely to be

481 absorbed by the leaf especially at low rainfall totals. In this case the multiple regression estimate of dry

482 deposition is underestimated by a factor equal to the efficiency with which dry deposition is absorbed

by the canopy. Implications for dry deposition absorption are discussed below in Sect. 4.1. 483

Dry deposition to the canopy is likely derived from ambient PM and not from resuspension of dust. The 484

485 7 Be: 210 Pb ratio of dry deposition to the canopy based on multiple regression coefficients =11 ±4, which is

486 comparable to our prior measurements of ambient PM10 (=10 ±2), and somewhat lower than openfall

wet deposition [flux-weighted average = 15.1 ±0.6; p=0.22], but significantly higher than bulk dry 487

488 deposition [=4.2 ±0.6, p<0.0001] (Landis et al., 2021). Deleted:

Deleted:)

Deleted: in throughfall versus

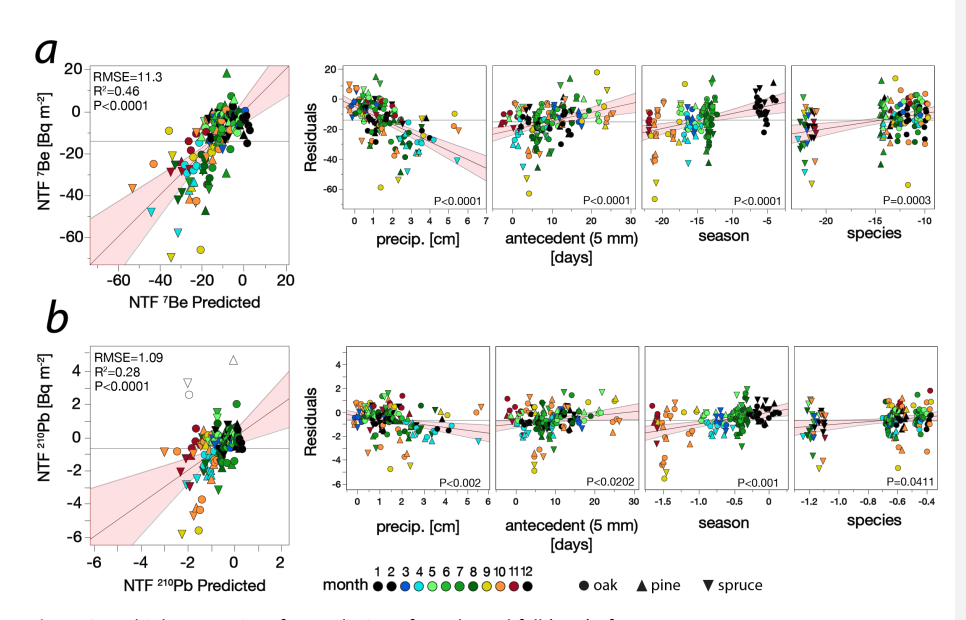


Figure 3. multiple regressions for prediction of net throughfall (NTF) of FRNs.
(a) ⁷Be and (b) ²¹⁰Pb. NTF is modeled with explanators including precipitation depth, antecedent dry period (since 5 mm precipitation), season, and tree species. Models are shown without transformation to retain interpretable units on the data but this does not impact significance of explanators. Three outliers omitted in ²¹⁰Pb regression are indicated with open symbols.

3.5. Importance of DOC and FPOM in MTE multiple regressions

For MTEs we similarly estimated dry deposition and canopy interactions that contribute to their enrichment in throughfall using multiple regression. All MTEs were found to have positive correlations with both antecedent dry period and rainfall depth (Table S1). Importantly, both FPOM and DOC contribute significantly to all FRN and MTE models. This suggests that carbon plays a significant role in release of both FRNs and MTEs from the canopy. DOC is the stronger explanator and typically supersedes FPOM in the model (Table S1). Because they have strong predictive power in FRN and MTE models, we also examined FPOM and DOC using multiple regression (Fig. 55). The FPOM model [R²=0.35] has significant explanators including season [19%], antecedent duration [11%], and rainfall depth [5%]. Surprisingly, there was no effect from species [p>0.05]. The strongest effect from antecedent duration uses a 15 mm rather than 5 mm precipitation threshold. Including DOC as an explanator strengthens the FPOM model [R² =0.58] as DOC becomes the strongest predictor [21%]. A model for DOC [R²=0.31] shows the same explanators as for FPOM, with season [14%], antecedent [7%], and rainfall depth [6%] each significant. DOC production is higher relative to FPOM in spring and fall [p<0.05], which is consistent with tree phenology and peak DOC production with both new foliar growth and senescence (Van Stan et al., 2012).

3.6. Dissolved Organic Carbon regulates FRN and MTE Net Throughfall

The coefficient θ_{DOC} obtained from multiple regression mass balance quantifies the increase in NTF per increase in DOC (µmol-MTE µmol-C⁻¹). This provides an empirical metric of FRN or MTE affinity for

| Deleted: s | |
|----------------------------|--|
| Deleted: models for | |
| Deleted: s | |
| Deleted: s | |
| Deleted: \$4 | |

throughfall DOC (Table S1). It can be expressed as an association constant (K_{DOC}) by normalizing each multiple regression coefficient by the average dissolved FRN or MTE concentration (μ mol L⁻¹). K_{DOC} is significantly correlated with EF across all elements, which supports the notion that DOC aids in regulating export of MTEs from the canopy (Fig. 4; R²=0.32, p=0.003; see also Hou et al., 2005 and Gandois et al., 2010). Moreover, there are additional noteworthy associations within the FRNs and MTEs. They are bound at lower EFs by group (1) consisting of 7 Be, 210 Pb, Be 7 , Pb 7 , Hg 7 , AI, and Fe [slope =0.381 ±0.056; R²=0.90, p=0.001]; these are elements with strongest oxide-over-humate preferences, and thus likely to be most weakly solubilized by DOC (Takahashi et al., 1999).

Separation of FRNs from their stable isotope counterparts within this relationship, with both lower K_{DOC} and lower EF, suggests that some age-dependence of PM regulates the metal-DOC association (Discussion S2, Fig. §8). Within the $^7Be-Be^T$ and $^{210}Pb-Pb^T$ pairs elemental chemistry is conserved, and differences in K_{DOC} and EF must be attributed to different PM ages/sources. The distinction made here is between secondary aerosol that characterizes 7Be and ^{210}Pb and resuspended dust or aged PM that more likely influences Be^T , Pb^T , (as well as Hg^T , Al, Fe, and U). Elsewhere we have described this as a particle-age effect to describe how PM metals become increasingly and irreversibly particulate-bound with increasing PM age (Landis et al., 2021b).

Deleted: S7

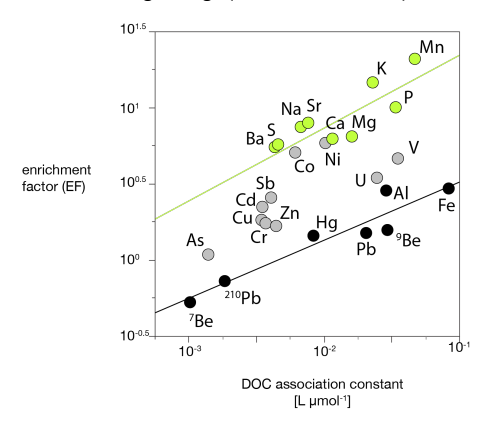


Figure 4. Dependence of throughfall EF on DOC binding constant, K_{DOC} .

 K_{DOC} was estimated as the increase in metal NTF per unit increase in DOC, normalized to metal concentration. Elements in black have large oxide (K_{OH}) over oxalate binding constants (K_{Ox}), elements in green have oxalate preference (Takahashi et al., 1999).

Alkaline and strongly cycled nutrient elements form a second boundary of group (2) elements at high EFs [slope =0.478 \pm 0.133; R²=0.72, p=0.0159]. The alkaline elements Ca, Sr and Ba have highest preference for humate over oxide ligands (Takahashi et al., 1999). K_{DOC} alone does not clearly separate groups 1 and 2 due, in part, to the particle age effect. This suggests that EF distinguishes metal source, with atmospheric deposition controlling group 1 and leaching controlling group 2. Trace metals in intermediate group (3) are increasingly likely to have metabolic contributions from canopy leaching with larger EFs.

3.7. PM storage, and change in storage (AS), in the forest canopy

 Our assumptions for FRN canopy mass balance underlying the derivation of Eq. 10 appear to be observed, with no detected differences in ^7Be and ^{210}Pb geochemical behaviors or rates of dry deposition. Lower $^7\text{Be}:^{210}\text{Pb}$ ratios and excess of ^{210}Pb over ^7Be in TF should thus be interpreted as a change in storage (ΔS) derived from within the non-metabolic materials of the $\frac{\text{tree}}{\text{canopy}}$. $^{210}\text{Pb}_{\Delta S}$ averaged 0.70 Bq m⁻² per storm or 29% of annual net throughfall flux. In contrast to net throughfall ($^{210}\text{Pb}_{\text{NTF}}$) which decreases with total precipitation, $^{210}\text{Pb}_{\Delta S}$ increases significantly with total precipitation at a rate of 0.22 ± 0.04 Bq m⁻² cm⁻¹, which is equivalent to 22 ± 4 Bq m⁻² per year [R²=0.19, p<0.0001]. $^{210}\text{Pb}_{\Delta S}$ was not influenced by antecedent dry period [r²=0.009, p=0.25], which lends confidence that $^{210}\text{Pb}_{\Delta S}$ does not simply reflect different depositional dynamics for ^7Be and ^{210}Pb . Multiple regression for $^{210}\text{Pb}_{\Delta S}$ yielded a strong model with significant, independent effects from rainfall depth [13%], species [9%], season [7%], and DOC [15%] [R²=0.46, n=137(8)] (Fig. 5). $^{210}\text{Pb}_{\Delta S}$ was highest in autumn and summer, and lowest in winter, irrespective of tree species and including the conifer species [p<0.05]. Spruce contributed larger change in storage than either pine or oak [p<0.05]. Linear, positive dependence on p_D demonstrates that $^{210}\text{Pb}_{\Delta S}$ supply is not readily exhausted as is the case for dry deposition (i.e., as shown in Fig. 2a).

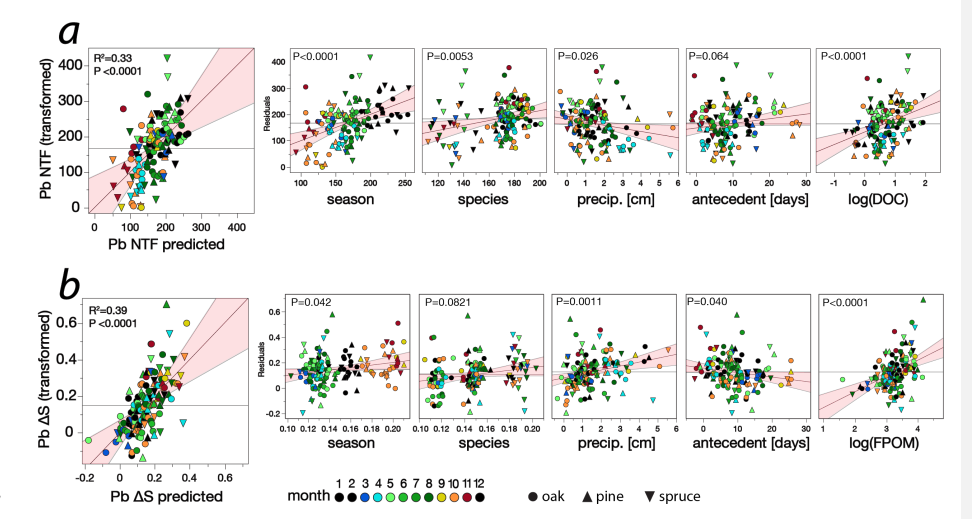


Figure 5. Multiple regressions for (a) 210 Pb net throughfall, (b) 210 Pb change in storage. Both variables are transformed to provide normal distributions.

When we compare regressions for $^{210}\text{Pb}_{\text{NTF}}$ and $^{210}\text{Pb}_{\Delta S}$, the importance of DOC is replaced by stronger correlation with FPOM in the ΔS model. In addition, where modeling of $^{210}\text{Pb}_{\text{NTF}}$ found no significant relationships with other metals, for the $^{210}\text{Pb}_{\Delta S}$ multiple regression multiple trace metals also provide explanatory power at the expense of season, DOC, and rainfall depth [R²=0.65, n=102(3)]. MTEs with strong explanatory power were $\text{Cu}_{\Delta S}$ [26%], $\text{Fe}_{\Delta S}$ [26%], $\text{Al}_{\Delta S}$ [24%], $\text{Pa}_{\Delta S}$ [22%] and $\text{Hg}_{\Delta S}$ [14%]. Correlation with Hg also removes autumn seasonality in $^{210}\text{Pb}_{\Delta S}$. These strong correlations among ΔS for multiple metals suggest that they are entrained in a common weathering process from the canopy. It is

577 important to note that ⁷Be_{NTF} provided no explanatory power in the ²¹⁰Pb_{ΔS} model [p=0.35], confirming the decoupling of ${}^{7}\text{Be}$ and ${}^{210}\text{Pb}_{\Delta S}$ through the mass balance model. 578 Deleted: expected 579 Among all MTEs, ΔS increases asymptotically with EF (Fig. 56). Sulfur is a notable exception because high Deleted: \$5 EF is attributable to dry deposition of gaseous SO_2 rather than ΔS . Change in storage was estimated for 580 MTEs as the relative contribution to annual NTF: $SO_4=7\%$; $^{210}Pb = 17\%$; Cd = 40%; $^{9}Be = 45\%$; As = 58%; 581 Hg = 60%; Pb = 63%; Fe =79%; Al = 79%; P =91% (Table S1). 582 583 4. Discussion 4.1 Verifying throughfall multiple-regression mass balances 584 585 Throughfall mass balances and the derivation of ΔS can be verified against ecosystem mass balance for Deleted: for the FRNs 586 the FRNs since, due to their short half-lives, the FRNs measured in vegetation and soil have unambiguous atmospheric sources. For example, long-term ²¹⁰Pb fluxes calculated from regional steady-587 state soil inventories average 173 ±24 Bq m⁻² y⁻¹ (n=8; (Landis et al., 2016, 2024b)). Long-term bulk 588 589 deposition measurements average 177 ±27 (n=12) but have decreased 4% per year from 2011 to 590 present and the most recent 4 years have averaged 158 ±26 (Landis et al., 2021). The sum of event-591 based W plus D fluxes estimated from multiple regression reported here over two years equates to 151 592 Bg m⁻² v⁻¹ which is somewhat lower than expected from soil inventories. However, the multiple 593 regression estimate of D assumes that dry deposition is fully removed by each subsequent precipitation event (Lovett and Lindberg, 1984). Our analysis of throughfall FRN concentrations in storms has already 594 595 shown that this is not correct (Fig. 2). Therefore, the multiple regression approach underestimates D and 596 thereby total annual deposition as well. From a whole tree mass balance approach (Landis, 2024b), an 597 absorption rate of D was estimated to be $\frac{49}{2}$ %, meaning the multiple regression underestimates D by a Deleted: for 598 factor of about 2. Adoption of this absorption factor hereafter requires a proportionate increase in Deleted: 53 annual dry deposition, almost doubling the estimate to 65 Bq m⁻² y⁻¹ and leading to an annual deposition 599 600 total of 174 Bq m⁻² y⁻¹. This more robust quantitation of dry deposition stands in better agreement with **Deleted:** estimate with correction to rates 601 soil records. The overall conclusion we reach is that both wet and dry deposition are well retained by the 602 forest canopy. FRNs also provide an opportunity to evaluate the suitability of conventional filtering throughfall mass 603 balance for MTEs. In contrast to the multiple-regression approach, the rate of ²¹⁰Pb dry deposition 604 605 predicted by the filtering approach (Eq. 4, with Al as reference) is higher by a factor of twelve, and total 606 annual ²¹⁰Pb deposition is higher by a factor of two over what is observed in local soils (360 Bg m⁻² y⁻¹). 607 The total ⁷Be flux predicted by filtering is higher than observed by a factor of 2.6 (4700 Bq m⁻²). The 608 filtering approach thus grossly overestimates secondary aerosol metal deposition, irrespective of 609 whether Na, Al or U are used as reference elements. These elements must therefore have substantial 610 contributions from canopy leaching or resuspended dust that do not impact FRNs and other secondary aerosol metals. Total rates of deposition for all MTEs estimated by the filtering approach are higher than 611 612 the multiple-regression approach on average by a factor of 5 (Discussion S3). 613 4.2. PM age and residence time in the phyllosphere Deleted: 7Be:210Pb ratios, The strongest control on ${}^{7}\text{Be:}^{210}\text{Pb}$ ratios in throughfall was tree species. We attribute this to an age 614 Deleted:,

17-times the ²¹⁰Pb annual flux in spruce (Landis, 2024b). Given these large estimates of ²¹⁰Pb storage in

effect and the storage of PM in phyllosphere by conifers with high foliar masses and LAI. Decreasing

This trend is also consistent with the size of total ²¹⁰Pb inventories likely to be stored in these trees based on whole-tree mass balance, increasing from 9-times the annual flux in oak, 11-times in pine, and

throughfall ⁷Be:²¹⁰Pb ratios in order oak > pine > spruce is consistent with characteristic leaf retention times of each species, about 6 months for oak, 1-2 years for white pine and up to 5-8 years for spruce.

615

616

617 618

the canopy, and assuming that the canopy is at steady-state with respect to inputs and export, the mean residence time of ²¹⁰Pb storage in the canopy (*S*) can be described as follows, with the corresponding analytical solution:

632
$$\frac{\partial S}{\partial t} = A - kS - \lambda S$$
 Eq. 15

633
$$S(t) = \frac{A}{k+\lambda} [1 - e^{-(k+\lambda) \cdot t}]$$
 Eq. 16

where S is canopy inventory (Bq m⁻²), A is the rate of canopy absorption of 210 Pb (which elsewhere is estimated as the product of wet and dry fluxes with their characteristic sorption coefficients of approximately 50% each, minus litter losses, summing to 57 Bq m⁻² y⁻¹ (Landis, 2024b)). Here λ is the 210 Pb decay constant, and k is a characteristic physicochemical weathering rate. k can be approximated if we observe a steady-state S =825 Bq m⁻² based on whole-tree measurements, which is an average for the two throughfall trees at the BM site. With these assumptions the mean residence time of PM metals in the phyllosphere with respect to weathering is 32 years (Fig. S-7). Independent age estimates of individual components of an adjacent red oak tree have also been made with 7 Be: 210 Pb chronometry for leaves (0.5 years), twigs (1.4 years), branches (7 years), moss (28 years), lichen (21 years), live surface (20-52 years), and bark (18 to >70 years). These ages are consistent with the superposition or ordering of, e.g, twig versus branch, and canopy crown versus tree base, and overall confirm that canopy storage of metals persists for decades (Landis, 2024b).

4.3. Implications for rates of MTE deposition to forest vegetation

The FRNs stand apart from MTEs in canopy mass balance, having EFs <1 and NTF that scales inversely with rainfall depth. What distinguishes the FRNs from other PM metals is radioactive decay, and the obvious cause for their diverging behaviors is a difference in characteristic ecosystem residence times. Whereas the FRNs are quintessential atmospheric metals and tracers of PM2.5, other trace metal cycles are therefore dominated by recycled pathways rather than novel PM deposition. This is illustrated clearly for the pairs ²¹⁰Pb versus Pb^T, and ⁷Be versus ⁹Be. Within each pair the FRN shows net sorption to the canopy while the stable isotope shows net release. Within each pair elemental chemistry must be conserved, and differences must therefore derive from half-life restrictions which in turn relate to different PM sources. In the absence of these insights from FRN mass balance, for example, large EFs for both ⁹Be and Pb^T in throughfall would be attributed to novel dry deposition rather than to a change in storage from recycled materials and legacy deposition. This has obvious consequences for estimating PM budgets and dry deposition by canopy mass balance, which may otherwise be overestimated by factors ranging from 2-10 (*Discussion S3*).

A critical question thus emerges: from where does a change in storage originate? Possible sources cannot be discriminated by our current methods but include resuspension of aged PM, e.g., dust, from the surrounding forest floor, as well as regional sources such as vehicular traffic and road dust; excretion of metabolic products from flora of the phyllosphere; or weathering of PM from legacy deposition to living and dead surfaces of the phyllosphere. For all MTEs, the strong dependence of both NTF and ΔS on DOC indicates that the immediate metal source is within the phyllosphere, Production of DOC in the phyllosphere in this case appears to act as a weathering mechanism, meaning that PM, metals, and dust are efficiently captured in the canopy, their constituents solubilized over some characteristic time frame that may span years to decades, likely altering their chemical speciation in association with organic carbon, and exporting them from the canopy in an operationally dissolved phase by DOC (Gandois et al., 2010; Roulier et al., 2021). Poorly soluble metals such as Fe and Al require solubilization by DOC to generate high throughfall EFs through ΔS (Hou et al., 2005). In conclusion, the strong correlations of ΔS among many TMs suggest that ΔS may be an emergent ecosystem property through which metal,

Deleted: aerosol

Deleted: S6

Deleted: or superposition

Deleted: particulate matter

Deleted: rather than surrounding ecosystem

Deleted: is

carbon, and hydrologic cycles converge (Van Stan and Stubbins, 2018). The phyllosphere thus plays a critical role in regulating timing, bioavailability, and reactivity of metals and carbon subsequently transferred to underlying soils. Future work should aim to extend the FRN mass balance to additional biomes and climate gradients so that the importance of phyllosphere storage for PM dynamics can be evaluated on a global scale in a context of climate change.

The role of organic particulate matter or FPOM is important in all MTE canopy cycles and warrants greater attention in future throughfall mass balance (Van Stan et al., 2021). Including the FPOM fraction in mass budgets increases the net throughfall of each MTE on average by 26%, but this number is higher for particle reactive elements including Hg (73%) or Pb (45%). Export of FPOM from the canopy mirrors processes that we observe for all MTEs. Its dependence on both precipitation and antecedent dry period, in turn, obscures the impact of these factors on MTEs which would otherwise be attributed to either leaching or novel dry deposition, respectively. Canopy FPOM export is highly seasonal, peaking strongly in summer to reflect productivity of the biological engine in the canopies of all tree species measured here (notably, both deciduous and coniferous). The production of FPOM via herbivory likely plays an important role (Frost and Hunter, 2004; Michalzik and Stadler, 2005). FPOM moreover figures directly in predictive models for DOC export and may thus represent a source of soluble carbon. As such, FPOM and DOC together influence trace metal cycling in the canopy and unite many trace metals in carbon cycling within the phyllosphere.

4.4. Implications of aerosol ΔS for trace metal throughfall budgets

PM storage in the forest canopy introduces complexity to metal exchange processes that control throughfall mass balance. Our compilation of literature TM throughfall highlights the widely varying behaviors of individual metals to transit through the forest canopy, ranging from strong net sorption to strong net release (Fig. 1). This variation is unlikely to result from elemental solubility behavior, metabolic cycling, or the vagaries of event-scale interaction between precipitation and canopy. Instead, we suggest that throughfall export from the canopy reflects the complexity of aerosol sources, how these have changed through time in both source strength and PM characteristics (Cho et al., 2011), and transformations that occur during PM residence both in the canopy and underlying forest soil. Thus, time and history are critical determinants in throughfall metal measurements.

With global anthropogenic emissions of many metals reduced in recent decades through emissions controls, the canopy is unlikely to be in steady-state with contemporary atmospheric deposition. Throughfall is thus likely to be a biased metric of deposition if a change in storage from prior deposition cannot be assessed. Future insights into the storage and solubilization of aerosol metals in the phyllosphere will require a combination of approaches to unravel varying sources and timescales of aerosol deposition to the canopy. We suggest that FRN mass balance and micrometeorology methods for, e.g., Hg deposition, are complementary approaches that can combined to verify both PM depositional processes and fluxes (Landis et al., 2024b). Here we have shown that multiple-regression mass balance, coupled with new FRN mass balance, and in combination whole-tree measurements (Landis, 2024b), can accurately quantify both new PM and TM deposition and their release from long-term storage. We anticipate that coupling throughfall, whole-tree mass balances, and FRN chronometry with stable isotope systems of, e.g., Cd, Cu, Pb, Hg, will yield new insights into metal dynamics in forest canopies and should be a focus of future efforts to understand fate and redistribution of atmospherically-derived metals.

Deleted: , as well,

Deleted: particulate matter

Deleted: in generation of FPOM

Deleted: trace metal

Deleted: EFs

Deleted: aerosol

Deleted: of old PM

Deleted: a

| 731 | Data Availability | |
|--|---|--|
| 732 733 734 | The data prepared for this manuscript are freely available to the public [Landis, Joshua (2025), "Throughfall mass balance with fallout radionuclides and major/trace elements", Mendeley Data, V1, doi: 10.17632/r9kpgp76xh.1]. | |
| 735 | | |
| 736 | Supplementary Materials | |
| 737 | Supplementary Materials supporting this manuscript are available at the publisher website. | |
| 738 | Author Contributions | |
| 739 | This work was completed wholly by JDL in the course of Ph.D dissertation research. | |
| 740 | | |
| 741 | Competing Interests | |
| 742 | The author declares that no competing interests influenced the conduct or conclusions of this research. | |
| 743 | | |
| 744 | Acknowledgements | |
| 745 746 747 748 749 750 | Thanks to Carl Renshaw (Dartmouth College) for constructive comments on an earlier version of this manuscript. DOC was measured with assistance from Caitlin Hicks Pries (Dartmouth College). Special thanks to Brian Jackson and the Dartmouth TEA Core facility for access to QQQ-ICPMS instrumentation. Special thanks to Vivien Taylor (Dartmouth College) for assistance with Hg measurements. Radionuclide measurements were performed in the Fallout Radionuclide Analytics facility (FRNA) at Dartmouth College, www.sites.dartmouth/frna/. | |
| 751 | | |
| 752 | Financial Support | |
| 753 | This work was supported financially by the Dept. of Earth Sciences at Dartmouth College. | |

- 754 References
- Ali, N., Khan, E. U., Akhter, P., Rana, M. A., Rajput, M. U., Khattak, N. U., Malik, F., and Hussain, S.: Wet
- 756 depositional fluxes of 210Pb- and 7Be-bearing aerosols at two different altitude cities of North Pakistan,
- 757 Atmos Environ, 45, 5699–5709, https://doi.org/10.1016/j.atmosenv.2011.07.032, 2011.
- 758 Atteia, O. and Dambrine, É.: Dynamique d'éléments traces dans les précipitations sous le couvert de 2
- 759 pessières peu polluées de Suisse romande, Annales des Sciences Forestières, 50, 445–459,
- 760 https://doi.org/10.1051/forest:19930503, 1993.
- 761 Avila, A. and Rodrigo, A.: Trace metal fluxes in bulk deposition, throughfall and stemflow at two evergreen
- 762 oak stands in NE Spain subject to different exposure to the industrial environment, Atmos Environ, 38, 171-
- 763 180, https://doi.org/10.1016/j.atmosenv.2003.09.067, 2004.
- 764 Barthlott, W. and Neinhuis, C.: Purity of the sacred lotus, or escape from contamination in biological surfaces,
- 765 Planta, 202, 1-8, 1997.
- 766 Bishop, K., Shanley, J. B., Riscassi, A., de Wit, H. A., Eklöf, K., Meng, B., Mitchell, C., Osterwalder, S., Schuster,
- 767 P. F., Webster, J., and Zhu, W.: Recent advances in understanding and measurement of mercury in the
- 768 environment: Terrestrial Hg cycling, Science of the Total Environment, 721,
- 769 https://doi.org/10.1016/j.scitotenv.2020.137647, 2020.
- 770 Böhlke, J. K. and Michel, R. L.: Contrasting residence times and fluxes of water and sulfate in two small
- 771 forested watersheds in Virginia, USA, Science of the Total Environment, 407, 4363–4377,
- 772 https://doi.org/10.1016/j.scitotenv.2009.02.007, 2009.
- 773 Bortolazzi, A., Da Ros, L., Rodeghiero, M., Tognetti, R., Tonon, G., and Ventura, M.: The canopy layer, a
- 5774 biogeochemical actor in the forest N-cycle, Science of the Total Environment, 576,
- 775 https://doi.org/10.1016/j.scitotenv.2021.146024, 2021.
- 776 Bringmark, L., Lundin, L., Augustaitis, A., Beudert, B., Dieffenbach-Fries, H., Dirnböck, T., Grabner, M. T.,
- 777 Hutchins, M., Kram, P., Lyulko, I., Ruoho-Airola, T., and Vana, M.: Trace metal budgets for forested
- 778 catchments in Europe-Pb, Cd, Hg, Cu and Zn, Water Air Soil Pollut, 224, https://doi.org/10.1007/s11270-013-
- 779 1502-8, 2013.
- 780 Chamberlain, A. C.: Interception and retention of radioactive aerosols by vegetation, Atmos Environ, 4, 57–
- 781 78, 1970.
- 782 Cho, S. H., Richmond-Bryant, J., Thornburg, J., Portzer, J., Vanderpool, R., Cavender, K., and Rice, J.: A
- 783 literature review of concentrations and size distributions of ambient airborne Pb-containing particulate
- 784 matter, Atmos Environ, 45, 5005–5015, https://doi.org/10.1016/j.atmosenv.2011.05.009, 2011.
- Demers, J. D., Driscoll, C. T., Fahey, T. J., and Yavitt, J. B.: Mercury cycling in litter and soil in different forest
- 786 types in the Adirondack region, New York, USA, Ecological Applications, 17, 1341–1351,
- 787 https://doi.org/10.1890/06-1697.1, 2007.
- 788 Draaijers, G. P. J., Erisman, J. W., Sprangert, T., and Wyers, G. P.: The application of measurements for
- 789 atmospheric deposition monitoring, Atmos Environ, 30, 3349–3361, 1996.
- 790 Duce, R. A., Hoffman, G. L., and Zoller, W. H.: Atmospheric Trace Metals at Remote Northern and Southern
- 791 Hemisphere Sites: Pollution or Natural?, Science (1979), 187, 60–61, 1975.
- 792 Eisalou, H. K., Şengönül, K., Gökbulak, F., Serengil, Y., and Uygur, B.: Effects of forest canopy cover and floor
- 793 on chemical quality of water in broad leaved and coniferous forests of Istanbul, Turkey, For Ecol Manage,
- 794 289, 371–377, https://doi.org/10.1016/j.foreco.2012.10.031, 2013.

- 795 Emerson, E. W., Katich, J. M., Schwarz, J. P., McMeeking, G. R., and Farmer, D. K.: Direct Measurements of
- 796 Dry and Wet Deposition of Black Carbon Over a Grassland, Journal of Geophysical Research: Atmospheres,
- 797 123, 12,277-12,290, https://doi.org/10.1029/2018JD028954, 2018.
- 798 Emerson, E. W., Hodshire, A. L., DeBolt, H. M., Bilsback, K. R., Pierce, J. R., McMeeking, G. R., and Farmer, D.
- 799 K.: Revisiting particle dry deposition and its role in radiative effect estimates, Proc Natl Acad Sci U S A, 117,
- 800 26076–26082, https://doi.org/10.1073/pnas.2014761117, 2020.
- 801 Farmer, D. K., Boedicker, E. K., and Debolt, H. M.: Dry Deposition of Atmospheric Aerosols: Approaches,
- 802 Observations, and Mechanisms, Annu Rev Phys Chem, https://doi.org/10.1146/annurev-physchem-090519,
- 803 2021.
- 804 Farmer, J. G., Eades, L. J., Graham, M. C., Cloy, J. M., and Bacon, J. R.: A comparison of the isotopic
- 805 composition of lead in rainwater, surface vegetation and tree bark at the long-term monitoring site,
- 806 Glensaugh, Scotland, in 2007, Science of the Total Environment, 408, 3704–3710,
- 807 https://doi.org/10.1016/j.scitotenv.2010.03.050, 2010.
- 808 Forti, M. C., Bicudo, D. C., Bourotte, C., De Cicco, V., and Arcova, F. C. S.: Rainfall and throughfall chemistry in
- 809 the Atlantic Forest: a comparison between urban and natural areas (São Paulo State, Brazil), Hydrol Earth Syst
- 810 Sci, 9, 570-585, 2005.
- 811 Frost, C. J. and Hunter, M. D.: Insect canopy herbivory and frass deposition affect soil nutrient dynamics and
- 812 export in oak mesocosms, Ecology, 85, 3335–3347, https://doi.org/10.1890/04-0003, 2004.
- Fu, X. W., Feng, X., Dong, Z. Q., Yin, R. S., Wang, J. X., Yang, Z. R., and Zhang, H.: Atmospheric gaseous
- 814 elemental mercury (GEM) concentrations and mercury depositions at a high-altitude mountain peak in south
- 815 China, Atmos Chem Phys, 10, 2425–2437, https://doi.org/10.5194/acp-10-2425-2010, 2010.
- 816 Gandois, L., Tipping, E., Dumat, C., and Probst, A.: Canopy influence on trace metal atmospheric inputs on
- forest ecosystems: Speciation in throughfall, Atmos Environ, 44, 824–833,
- 818 https://doi.org/10.1016/j.atmosenv.2009.11.028, 2010.
- 819 Graydon, J. A., St. Louis, V. L., Hintelmann, H., Lindberg, S. E., Sandilands, K. A., Rudd, J. W. M., Kelly, C. A.,
- 820 Hall, B. D., and Mowat, L. D.: Long-term wet and dry deposition of total and methyl mercury in the remote
- 821 boreal ecoregion of Canada, Environ Sci Technol, 42, 8345–8351, https://doi.org/10.1021/es801056j, 2008.
- 622 Graydon, J. A., St. Louis, V. L., Hintelmann, H., Lindberg, S. E., Sandilands, K. A., Rudd, J. W. M., Kelly, C. A.,
- 823 Tate, M. T., Krabbenhoft, D. P., and Lehnherr, I.: Investigation of uptake and retention of atmospheric Hg(II)
- 824 by boreal forest plants using stable Hg isotopes, Environ Sci Technol, 43, 4960–4966,
- 825 https://doi.org/10.1021/es900357s, 2009.
- 826 Grigal, D. F., Kolka, R. K., Fleck, J. A., and Nater, E. A.: Mercury budget of an upland-peatland watershed,
- 827 Biogeochemistry, 50, 95–109, https://doi.org/10.1023/A:1006322705566, 2000.
- 828 Gründel, M. and Porstendörfer, J.: Differences between the activity size distributions of the different natural
- 829 radionuclide aerosols in outdoor air, Atmos Environ, 38, 3723–3728,
- 830 https://doi.org/10.1016/j.atmosenv.2004.01.043, 2004.
- 831 Henderson, G. S., Harris, W. F., Todd, D. E., and Grizzard, T.: Quantity and Chemistry of Throughfall as
- 832 Influenced by Forest-Type and Season, Source: Journal of Ecology, 365–374 pp., 1977.
- 833 Hicks, B. B.: MEASURING DRY DEPOSITION: A RE-ASSESSMENT OF THE STATE OF THE ART, 1986.
- 834 Hicks, B. B., Saylor, R. D., and Baker, B. D.: Journal of geophysical research, Journal of Geophysical Research:
- 835 Atmospheres, 121, 14691–14707, https://doi.org/10.1038/175238c0, 2016.

- 836 Hosker, R. P. and Lindberg, S. E.: Review: Atmospheric deposition and plant assimilation of gases and
- 837 particles, Atmospheric Environment (1967), 16, 889–910, https://doi.org/10.1016/0004-6981(82)90175-5,
- 838 1982.
- 839 Hou, H., Takamatsu, T., Koshikawa, M. K., and Hosomi, M.: Trace metals in bulk precipitation and throughfall
- in a suburban area of Japan, Atmos Environ, 39, 3583–3595,
- 841 https://doi.org/10.1016/j.atmosenv.2005.02.035, 2005.
- 842 Huang, J. H., Ilgen, G., and Matzner, E.: Fluxes and budgets of Cd, Zn, Cu, Cr and Ni in a remote forested
- 843 catchment in Germany, Biogeochemistry, 103, 59–70, https://doi.org/10.1007/s10533-010-9447-0, 2011.
- 844 IAEA: Quantification of radionuclide transfer in terrestrial and freshwater environments., IAEA-Techdoc-1616,
- 845 Vienna, 671-4 pp., https://doi.org/10.1016/j.jenvrad.2009.06.021, 2009.
- 846 IPCC: Climate Change 2021: The Physical Science Basis, International Panel on Climate Change, 3–3 pp.,
- 847 https://doi.org/10.3724/sp.j.7103161536, 2021.
- 848 Iverfeldt, Å.: Mercury in forest canopy throughfall water and its relation to atmospheric deposition, Water Air
- 849 Soil Pollut, 56, 553–564, https://doi.org/10.1007/BF00342299, 1991.
- 850 Jaenicke, R.: NATURAL AEROSOLS, Ann N Y Acad Sci, 338, 317–329, https://doi.org/10.1111/j.1749-
- 851 6632.1980.tb17129.x, 1980.
- 852 Jiskra, M., Sonke, J. E., Obrist, D., Bieser, J., Ebinghaus, R., Myhre, C. L., Pfaffhuber, K. A., Wängberg, I.,
- 853 Kyllönen, K., Worthy, D., Martin, L. G., Labuschagne, C., Mkololo, T., Ramonet, M., Magand, O., and
- 854 Dommergue, A.: A vegetation control on seasonal variations in global atmospheric mercury concentrations,
- 855 Nat Geosci, 11, 244–250, https://doi.org/10.1038/s41561-018-0078-8, 2018.
- Johnson, A. H. and Siccama, T. G.: Acid deposition and forest decline, Environ Sci Technol, 17,
- 857 https://doi.org/10.1021/es00113a001, 1983.
- 858 Karwan, D. L., Siegert, C. M., Levia, D. F., Pizzuto, J., Marquard, J., Aalto, R., and Aufdenkampe, A. K.:
- 859 Beryllium-7 wet deposition variation with storm height, synoptic classification, and tree canopy state in the
- $860 \qquad \text{mid-Atlantic USA, Hydrol Process, 30, 75-89, https://doi.org/10.1002/hyp.10571, 2016.}$
- Karwan, D. L., Pizzuto, J. E., Aalto, R., Marquard, J., Harpold, A., Skalak, K., Benthem, A., Levia, D. F., Siegert, C.
- 862 M., and Aufdenkampe, A. K.: Direct Channel Precipitation and Storm Characteristics Influence Short-Term
- 863 Fallout Radionuclide Assessment of Sediment Source, Water Resour Res, 54, 4579–4594,
- 864 https://doi.org/10.1029/2017WR021684, 2018.
- 865 Kato, H., Onda, Y., and Gomi, T.: Interception of the Fukushima reactor accident-derived 137Cs, 134Cs and
- 866 131I by coniferous forest canopies, Geophys Res Lett, 39, 1-6, https://doi.org/10.1029/2012GL052928, 2012.
- 867 Koch, D. M., Jacob, D. J., and Graustein, W. C.: Vertical transport of tropospheric aerosols as indicated by 7Be
- 868 and 210Pb in a chemical tracer model, Journal of Geophysical Research Atmospheres, 101, 18651–18666,
- 869 https://doi.org/10.1029/96jd01176, 1996.
- 870 Kolka, R. K., Nater, E. A., Grigal, D. F., and Verry, E. S.: Atmospheric inputs of mercury and organic carbon into
- a forested upland/bog watershed, Water Air Soil Pollut, 113, 273–294,
- 872 https://doi.org/10.1023/A:1005020326683, 1999.
- 873 Kopáček, J., Turek, J., Hejzlar, J., and Šantrůčková, H.: Canopy leaching of nutrients and metals in a mountain
- 874 spruce forest, Atmos Environ, 43, 5443–5453, https://doi.org/10.1016/j.atmosenv.2009.07.031, 2009.
- 875 Laguionie, P., Roupsard, P., Maro, D., Solier, L., Rozet, M., Hébert, D., and Connan, O.: Simultaneous
- 876 quantification of the contributions of dry, washout and rainout deposition to the total deposition of particle-

- 877 bound 7Be and 210Pb on an urban catchment area on a monthly scale, J Aerosol Sci, 77, 67–84,
- 878 https://doi.org/10.1016/j.jaerosci.2014.07.008, 2014.
- 879 Lamborg, C. H., Engstrom, D. R., Fitzgerald, W. F., and Balcom, P. H.: Apportioning global and non-global
- 880 components of mercury deposition through (210)Pb indexing., Sci Total Environ, 448, 132–40,
- 881 https://doi.org/10.1016/j.scitotenv.2012.10.065, 2013.
- 882 Landis, J. D.: Age-Dating of Foliage and Soil Organic Matter: Aligning 228Th:228Ra and 7Be:210Pb
- 883 Radionuclide Chronometers over Annual to Decadal Time Scales, Environ Sci Technol, 57, 15047–15054,
- 884 https://doi.org/10.1021/acs.est.3c06012, 2023.
- 885 Landis, J. D.: Accumulation of atmospheric metals in natural vegetation, Chapter 4 in Terrestrial Exchange of
- 886 Atmospheric Metals: Insights from Fallout Radionuclides, PhD, Dartmouth College, Hanover, NH, 2024a.
- 887 Landis, J. D.: Whole-tree mass balance of fallout radionuclides and atmospheric metals, Chapter 6 in
- 888 Terrestrial Exchange of Atmospheric Metals: Insights from Fallout Radionuclides, PhD, Dartmouth College,
- 889 Hanover, 240–267 pp., 2024b.
- 890 Landis, J. D.: Throughfall mass balance with fallout radionuclides and major/trace elements, Mendeley
- 891 Data, V1, doi: 10.17632/r9kpgp76xh.1, 2025.
- 892 Landis, J. D., Renshaw, C. E., and Kaste, J. M.: Measurement of 7Be in soils and sediments by gamma
- 893 spectroscopy, Chem Geol, 291, 175–185, https://doi.org/10.1016/j.chemgeo.2011.10.007, 2012.
- 894 Landis, J. D., Renshaw, C. E., and Kaste, J. M.: Quantitative retention of atmospherically deposited elements
- 895 by native vegetation is traced by the fallout radionuclides 7Be and 210Pb, Environ Sci Technol, 48, 12022–
- 896 12030, https://doi.org/10.1021/es503351u, 2014.
- 897 Landis, J. D., Renshaw, C. E., and Kaste, J. M.: Beryllium-7 and lead-210 chronometry of modern soil
- 898 processes: The Linked Radionuclide aCcumulation model, LRC, Geochim Cosmochim Acta, 180, 109–125,
- 899 https://doi.org/10.1016/j.gca.2016.02.013, 2016.
- 900 Landis, J. D., Feng, X., Kaste, J. M., and Renshaw, C. E.: Aerosol populations, processes and ages contributing
- 901 to bulk atmospheric deposition: insights from a 9-year study of 7Be, 210Pb, sulfate and major/trace
- 902 elements, Journal of Geophysical Research: Atmospheres, 2021a.
- 903 Landis, J. D., Renshaw, C. E., and Kaste, J. M.: Sorption Behavior and Aerosol-Particulate Transitions
- 904 of 7Be, 10Be, and 210Pb: A Basis for Fallout Radionuclide Chronometry, Environ Sci Technol, 55, 14957–14967,
- 905 https://doi.org/10.1021/acs.est.1c03194, 2021b.
- 906 Landis, J. D., Taylor, V. F., Hintelmann, H., and Hrenchuk, L. E.: Predicting behavior and fate of atmospheric
- 907 mercury in soils: age-dating METAALICUS Hg isotope spikes with fallout radionuclide chronometry,
- $908 \qquad \hbox{Environmental Science and Technology, in print, 2024a}.$
- 909 Landis, J. D., Obrist, D., Zhou, J., Renshaw, C. E., McDowell, W. H., Nytch, C. J., Palucis, M. C., Del Vecchio, J.,
- 910 Lopez, F. M., and Taylor, V. F.: Quantifying soil accumulation of atmospheric mercury using fallout
- 911 radionuclide chronometry, Nat Commun, 15, 5430, 2024b.
- 912 Landre, A. L., Watmough, S. A., and Dillon, P. J.: The effects of dissolved organic carbon, acidity and
- 913 seasonality on metal geochemistry within a forested catchment on the Precambrian Shield, central Ontario,
- 914 Canada, Biogeochemistry, 93, 271–289, https://doi.org/10.1007/s10533-009-9305-0, 2009.
- 915 Larssen, T., de Wit, H. A., Wiker, M., and Halse, K.: Mercury budget of a small forested boreal catchment in
- 916 southeast Norway, Science of the Total Environment, The, 404, 290–296, 2008.

- 917 Lawson, N. M. and Mason, R. P.: Concentration of mercury, methylmercury, cadmium, lead, arsenic, and
- 918 selenium in the rain and stream water of two contrasting watersheds in western Maryland, Water Res, 35,
- 919 4039–4052, https://doi.org/10.1016/S0043-1354(01)00140-3, 2001.
- 920 Lindberg, S. E. and Harriss, R. C.: THE ROLE OF ATMOSPHERIC DEPOSITION IN AN EASTERN U.S. DECIDUOUS
- 921 FOREST, Water Air Soil Pollut, 16, 13–31, 1981.
- 922 Lindberg, S. E., Harriss, R. C., and Turner, R. R.: Atmospheric deposition of metals to forest vegetation,
- 923 Science (1979), 216, 1609–1611, https://doi.org/10.1126/science.215.4540.1609, 1982.
- 924 Liu, H., Considine, D. B., Horowitz, L. W., Crawford, J. H., Rodriguez, J. M., Strahan, S. E., Damon, M. R.,
- 925 Steenrod, S. D., Xu, X., Kouatchou, J., Carouge, C., and Yantosca, R. M.: Using beryllium-7 to assess cross-
- 926 tropopause transport in global models, Atmos Chem Phys, 16, 4641–4659, https://doi.org/10.5194/acp-16-
- 927 4641-2016, 2016.
- 928 St. Louis, V. L., Rudd, J. W. M., Kelly, C. A., Hall, B. D., Rolfhus, K. R., Scott, K. J., Lindberg, S. E., and Dong, W.:
- 929 Importance of the forest canopy to fluxes of methyl mercury and total mercury to boreal ecosystems, Environ
- 930 Sci Technol, 35, 3089–3098, https://doi.org/10.1021/es001924p, 2001.
- 931 St. Louis, V. L., Graydon, J. A., Lehnherr, I., Amos, H. M., Sunderland, E. M., St. Pierre, K. A., Emmerton, C. A.,
- 932 Sandilands, K., Tate, M., Steffen, A., and Humphreys, E. R.: Atmospheric concentrations and wet/dry loadings
- 933 of mercury at the remote experimental lakes area, northwestern ontario, Canada, Environ Sci Technol, 53,
- 934 8017–8026, https://doi.org/10.1021/acs.est.9b01338, 2019.
- 935 Lovett, G. M. and Lindberg, S. E.: Dry Deposition and Canopy Exchange in a Mixed Oak Forest as Determined
- 936 by Analysis of Throughfall, J Appl Ecol, 21, 1013, https://doi.org/10.2307/2405064, 1984.
- 937 Luo, X., Bing, H., Luo, Z., Wang, Y., and Jin, L.: Impacts of atmospheric particulate matter pollution on
- 938 environmental biogeochemistry of trace metals in soil-plant system: A review, Environmental Pollution, 255,
- 939 https://doi.org/10.1016/j.envpol.2019.113138, 2019.
- 940 Mahendrappa, M. K.: Tree species and urea treatment effects on sulfur and metals in throughfall and
- stemflow of some eastern Canadian forest stands, Canadian Journal of Forestry Research, 17, 1035–1042,
- 942 1987.
- 943 Mahowald, N. M., Hamilton, D. S., Mackey, K. R. M., Moore, J. K., Baker, A. R., Scanza, R. A., and Zhang, Y.:
- 944 Aerosol trace metal leaching and impacts on marine microorganisms, Nat Commun, 9,
- 945 https://doi.org/10.1038/s41467-018-04970-7, 2018.
- 946 Malek, S. and Astel, A.: Throughfall chemistry in a spruce chronosequence in southern Poland, Environmental
- 947 Pollution, 155, 517–527, https://doi.org/10.1016/j.envpol.2008.01.031, 2008.
- 948 Matschullat, J., Maenhaut, W., Zimmermann, F., and Juliane Fiebig: Aerosol and bulk deposition trends in the
- 949 1990's, Eastern Erzgebirge, Central Europe, Atmos Environ, 34, 3213-3221, https://doi.org/10.1016/S1352-
- 950 2310(99)00516-6, 2000.
- 951 McDowell, W. H., Pérez-Rivera, K. X., and Shaw, M. E.: Assessing the Ecological Significance of Throughfall in
- 952 Forest Ecosystems, 299–318, https://doi.org/10.1007/978-3-030-26086-6_13, 2020.
- 953 Michalzik, B. and Stadler, B.: Importance of canopy herbivores to dissolved and particulate organic matter
- 954 fluxes to the forest floor, in: Geoderma, 227–236, https://doi.org/10.1016/j.geoderma.2004.12.006, 2005.
- 955 Michopoulos, P., Baloutsos, G., Economou, A., Nikolis, N., Bakeas, E. B., and Thomaidis, N. S.:
- 956 Biogeochemistry of lead in an urban forest in Athens, Greece, Biogeochemistry, 73, 345–357,
- 957 https://doi.org/10.1007/s10533-004-0359-8, 2005.

- 958 Michopoulos, P., Bourletsikas, A., Kaoukis, K., Daskalakou, E., Karetsos, G., Kostakis, M., Thomaidis, N. S.,
- 959 Pasias, I. N., Kaberi, H., and Iliakis, S.: The distribution and variability of heavy metals in a mountainous fir
- 960 forest ecosystem in two hydrological years, Global Nest Journal, 20, 188–197,
- 961 https://doi.org/10.30955/gnj.002506, 2018.
- 962 Miller, C. and Hoffman, F.: An examination of the environmental half-time for radionuclides deposited on
- 963 vegetation., Health Phys, 45, 731–744, 1983.
- Obrist, D., Roy, E. M., Harrison, J. L., Kwong, C. F., William Munger, J., Moosmüller, H., Romero, C. D., Sun, S.,
- 965 Zhou, J., and Commane, R.: Previously unaccounted atmospheric mercury deposition in a midlatitude
- 966 deciduous forest, Proc Natl Acad Sci U S A, 118, https://doi.org/10.1073/pnas.2105477118, 2021.
- 967 Oziegbe, M. B., Muoghalu, J. I., and Oke, S. O.: Litterfall, precipitation and nutrient fluxes in a secondary
- 968 lowland rain forest in Ile-Ife, Nigeria, Acta Bot Brasilica, 25, 664–671, https://doi.org/10.1590/s0102-
- 969 33062011000300020, 2011.
- 970 Petty, W. H. and Lindberg, S. E.: A intensive 1-month investigation of trace metal deposition and throughfall
- at a mountain spruce forest, Water Air Soil Pollut, 53, 213–226, 1990.
- 972 PRISM Climate Group, Oregon State University, https://prism.oregonstate.edu, data created 4 Feb 2014:
- 973 Pryor, S. C., Barthelmie, R. J., Larsen, S. E., and Sørensen, L. L.: Ultrafine particle number fluxes over and in a
- 974 deciduous forest, J Geophys Res, 122, 405–422, https://doi.org/10.1002/2016JD025854, 2017.
- 975 Rea, A. W., Lindberg, S. E., and Keeler, G. J.: Dry deposition and foliar leaching of mercury and selected trace
- 976 elements in deciduous forest throughfall, Atmos Environ, 35, 3453–3462, https://doi.org/10.1016/S1352-
- 977 2310(01)00133-9, 2001.
- 978 Rea, A. W., Lindberg, S. E., Scherbatskoy, T., and Keeler, G. J.: Mercury accumulation in foliage over time in
- 979 two northern mixed-hardwood forests, Water Air Soil Pollut, 133, 49–67,
- 980 https://doi.org/10.1023/A:1012919731598, 2002.
- 981 Rehmus, A., Bigalke, M., Boy, J., Valarezo, C., and Wilcke, W.: Aluminum cycling in a tropical montane forest
- $982 \qquad ecosystem \ in \ southern \ Ecuador, \ Geoderma, \ 288, \ 196-203, \ https://doi.org/10.1016/j.geoderma.2016.11.002, \ and \ an alternative \ an alternative \ and \ an alternative \ and \ an alternative \ an alternative \ an alternative \ an alternative \ and \ an alternative \ an alternative$
- 983 2017
- 984 Reich, P. B., Oleksyn, J., Modrzynski, J., and Tjoelker, M. G.: Evidence that longer needle retention of spruce
- and pine populations at high elevations and high latitudes is largely a phenotypic response, Tree Physiol, 16,
- 986 643–647, https://doi.org/10.1093/treephys/16.7.643, 1996.
- 987 Resongles, E., Dietze, V., Green, D. C., Harrison, R. M., Ochoa-Gonzalez, R., Tremper, A. H., and Weiss, D. J.:
- 988 Strong evidence for the continued contribution of lead deposited during the 20th century to the atmospheric
- 989 environment in London of today, Proceedings of the National Scademy of Sciences,
- $990 \qquad \text{https://doi.org/10.1073/pnas.2102791118/-/DCSupplemental, 2021.} \\$
- 991 Rodrigo, A., Avila, A., and Gomez-Bolea, A.: Trace metal contents in Parmelia caperata (L.) Ach. compared to
- 992 bulk deposition, throughfall and leaf-wash fluxes in two holm oak forests in Montseny (NE Spain), Atmos
- 993 Environ, 33, 359-367, 1999.
- 994 Roulier, M., Bueno, M., Coppin, F., Nicolas, M., Thiry, Y., Rigal, F., Pannier, F., and Le Hécho, I.: Atmospheric
- 995 iodine, selenium and caesium depositions in France: II. Influence of forest canopies, Chemosphere, 273,
- 996 https://doi.org/10.1016/j.chemosphere.2020.128952, 2021.

- 997 Russell, I. J., Choquette, C. E., Fang, S., Dundulis, W. P., Pao, A. A., and Pszenny, A. A. P.: Vegetation as a Sink
- 998 for Atmospheric Particulates: Quantitative Studies in Rain and Dry Deposition tests, J Geophys Res, 86, 5347–
- 999 5363, 1981.
- 1000 Saylor, R. D., Baker, B. D., Lee, P., Tong, D., Pan, L., and Hicks, B. B.: The particle dry deposition component of
- total deposition from air quality models: right, wrong or uncertain?, Tellus B Chem Phys Meteorol, 71, 1–22,
- 1002 https://doi.org/10.1080/16000889.2018.1550324, 2019.
- 1003 Schleppi, P., Conedera, M., Sedivy, I., and Thimonier, A.: Correcting non-linearity and slope effects in the
- estimation of the leaf area index of forests from hemispherical photographs, Agric For Meteorol, 144, 236–
- 1005 242, https://doi.org/10.1016/j.agrformet.2007.02.004, 2007.
- 1006 Schumacher, J. C.: Stratigraphy and geochemistry of the Ammonoosuc volcanics, central Massachusetts and
- 1007 southwestern New Hampshire, Am J Sci, 288, 619–663, 1988.
- 1008 Schwesig, D. and Matzner, E.: Pools and fluxes of mercury and methylmercury in two forested catchments in
- 1009 Germany, Science of the Total Environment, 260, 213–223, https://doi.org/10.1016/S0048-9697(00)00565-9,
- 1010 2000.
- 1011 Shahid, M., Dumat, C., Khalid, S., Schreck, E., Xiong, T., and Niazi, N. K.: Foliar heavy metal uptake, toxicity and
- detoxification in plants: A comparison of foliar and root metal uptake, J Hazard Mater, 325, 36–58,
- 1013 https://doi.org/10.1016/j.jhazmat.2016.11.063, 2017.
- 1014 Shanley, J. B.: Field measurements of dry deposition to spruce foliage and petri dishes in the black forest,
- 1015 F.R.G., Atmospheric Environment (1967), 23, 403–414, https://doi.org/10.1016/0004-6981(89)90586-6, 1989.
- 1016 Skrivan, P., Rusek, J., Fottova, D., Burian, M., and Minarik, L.: Factors affecting the content of heavy metals in
- 1017 bulk atmospheric precipitation, throughfall and stemflow in central Bohemia, Czech Republic, Water Air Soil
- 1018 Pollut, 85, 841-846, 1995.
- 1019 Sohrt, J., Uhlig, D., Kaiser, K., von Blanckenburg, F., Siemens, J., Seeger, S., Frick, D. A., Krüger, J., Lang, F., and
- 1020 Weiler, M.: Phosphorus Fluxes in a Temperate Forested Watershed: Canopy Leaching, Runoff Sources, and In-
- 1021 Stream Transformation, Frontiers in Forests and Global Change, 2, https://doi.org/10.3389/ffgc.2019.00085,
- 1022 2019.
- 1023 Stachurski, A. and Zimka, J. R.: Atmospheric input of elements to forest ecosystems: A method of estimation
- using artificial foliage placed above rain collectors, Environmental Pollution, 110, 345–356,
- 1025 https://doi.org/10.1016/S0269-7491(99)00290-0, 2000.
- 1026 Staelens, J., Houle, D., De Schrijver, A., Neirynck, J., and Verheyen, K.: Calculating dry deposition and canopy
- 1027 exchange with the canopy budget model: Review of assumptions and application to two deciduous forests,
- 1028 Water Air Soil Pollut, 191, 149–169, https://doi.org/10.1007/s11270-008-9614-2, 2008.
- 1029 Van Stan, J. T. and Pypker, T. G.: A review and evaluation of forest canopy epiphyte roles in the partitioning
- and chemical alteration of precipitation, https://doi.org/10.1016/j.scitotenv.2015.07.134, 1 December 2015.
- 1031 Van Stan, J. T. and Stubbins, A.: Tree-DOM: Dissolved organic matter in throughfall and stemflow, Limnol
- 1032 Oceanogr Lett, 3, 199–214, https://doi.org/10.1002/lol2.10059, 2018.
- 1033 Van Stan, J. T., Levia, D. F., Inamdar, S. P., Lepori-Bui, M., and Mitchell, M. J.: The effects of phenoseason and
- 1034 storm characteristics on throughfall solute washoff and leaching dynamics from a temperate deciduous
- forest canopy, Science of the Total Environment, 430, 48–58,
- 1036 https://doi.org/10.1016/j.scitotenv.2012.04.060, 2012.

- 1037 Van Stan, J. T., Ponette-González, A. G., Swanson, T., and Weathers, K. C.: Throughfall and stemflow are
- 1038 major hydrologic highways for particulate traffic through tree canopies, Front Ecol Environ, 19, 404–410,
- 1039 https://doi.org/10.1002/fee.2360, 2021.
- 1040 Sumerling, T. J.: The use of mosses as indicators of airborne radionuclides near a major nuclear installation,
- 1041 Science of The Total Environment, 35, 22, 1984.
- 1042 Takahashi, Y., Minai, Y., Ambe, S., Makide, Y., and Ambe, F.: Comparison of adsorption behavior of multiple
- 1043 inorganic ions on kaolinite and silica in the presence of humic acid using the multitracer technique, Geochim
- 1044 Cosmochim Acta, 63, 815–836, https://doi.org/10.1016/S0016-7037(99)00065-4, 1999.
- 1045 Tan, S., Zhao, H., Yang, W., Tan, B., Yue, K., Zhang, Y., Wu, F., and Ni, X.: Forest canopy can efficiently filter
- 1046 trace metals in deposited precipitation in a subalpine spruce plantation, Forests, 10,
- 1047 https://doi.org/10.3390/f10040318, 2019.
- 1048 Taylor, S. R. and McLennan, S. M.: The geochemical evolution of the continental crust,
- 1049 https://doi.org/10.1029/95RG00262, 1995.
- 1050 Taylor, V. F., Landis, J. D., and Janssen, S. E.: Tracing the sources and depositional history of mercury to
- 1051 coastal northeastern U.S. lakes, Environ Sci Process Impacts, 24, 1805–1820,
- 1052 https://doi.org/10.1039/d2em00214k, 2022.
- 1053 Thimonier, A., Sedivy, I., and Schleppi, P.: Estimating leaf area index in different types of mature forest stands
- 1054 in Switzerland: A comparison of methods, Eur J For Res, 129, 543-562, https://doi.org/10.1007/s10342-009-
- 1055 0353-8, 2010.
- 1056 Ukonmaanaho, L., Starr, M., Mannio, J., and Ruoho-Airola, T.: Heavy metal budgets for two headwater
- forested catchments in background areas of Finland, Environmental Pollution, 114, 63–75, 2001.
- 1058 Ulrich, B.: Interaction of Forest Canopies with Atmospheric Constituents: SO2, alkali and earth alkali cations
- and chloride, in: Effects of accumulation of air pollutants in forest ecosystems, edited by: Ulrich, B. and
- 1060 Pankrath, J., Spring, Dordrecht, The Netherlands, 33–45, 1983.
- 1061 USEPA, U. S. E. P. A.: Human Health Risk Assessment Protocol for Hazardous Waste Combustion Facilities
- 1062 Final This page deliberately left blank, EPA530-R-05-006, 2005.
- 1063 Wang, X., Yuan, W., Lin, C.-J., Luo, J., Wang, F., Feng, X., Fu, X., and Liu, C.: Underestimated sink of
- atmospheric mercury in a deglaciated forest chronosequence, Environ. Sci. Technol., 54, 8083–8093, 2020.
- 1065 WHO: Ambient air pollution: A global assessment of exposure and burden of disease, Geneva, 2016.
- 1066 WHO: WHO global air quality guidelines. Particulate matter (PM2.5 and PM10), ozone, nitrogen dioxide,
- 1067 sulfur dioxide and carbon monoxide., Geneva, 2021.
- 1068 Wilcke, W., Velescu, A., Leimer, S., Bigalke, M., Boy, J., and Valarezo, C.: Biological versus geochemical control
- and environmental change drivers of the base metal budgets of a tropical montane forest in Ecuador during
- 1070 15 years, Biogeochemistry, 136, 167–189, https://doi.org/10.1007/s10533-017-0386-x, 2017.
- 1071 Winkler, R., Dietl, F., Frank, G., and Tschiersch, J.: Temporal variation of 7Be and 210Pb size distributions in
- ambient aerosol, Atmos Environ, 32, 983–991, https://doi.org/10.1016/S1352-2310(97)00333-6, 1998.
- 1073 Wu, Y.-L., Davidson, C. I., LIndberg, S. E., and Russell, A. G.: Resuspension of Particulate Chemical Species at
- 1074 Forested Sites, Environ Sci Technol, 26, 2428–2435, https://doi.org/10.1021/es00036a014, 1992.
- 1075 Wyttenbach, A. and Tobler, L.: The seasonal variation of 20 elements in 1st and 2nd year needles of Norway
- 1076 spruce, Picea abies (L.) Karst, Trees, 2, 52–64, https://doi.org/10.1007/BF01196345, 1988.

| 1077 | Yamagata, N.: Contamination of leaves by radioactive fall-out, Nature, 198, 1220–1221, 1963. |
|--------------|--|
| 1078 1079 | Yamagata, N., Matsuda, S., and Chiba, M.: Radioecology of cesium-137 and strontium-90 in a forest, J Radiat Res, 10, 107–112, 1969. |
| 1080 1081 | Yang, H. and Appleby, P. G.: Use of lead-210 as a novel tracer for lead (Pb) sources in plants, Sci Rep, 6, 1–9, https://doi.org/10.1038/srep21707, 2016. |
| 1082 1083 | Yoshida, S. and Ichikuni, M.: Role of forest canopies in the collection and neutralization of airborne acid substances, The Science of the Total Environment, 35–43 pp., 1989. |
| 1084 1085 | Zhang, S. and Liang, C.: Effect of a native forest canopy on rainfall chemistry in China's Qinling Mountains, Environ Earth Sci, 67, 1503–1513, https://doi.org/10.1007/s12665-012-1594-2, 2012. |
| 1086 1087 | Zhou, J., Obrist, D., Dastoor, A., Jiskra, M., and Ryjkov, A.: Vegetation uptake of mercury and impacts on global cycling, https://doi.org/10.1038/s43017-021-00146-y, 1 April 2021. |